IEEE Access
Multidisciplinary | Rapid Review | Open Access Journal

Received 18 January 2024, accepted 23 January 2024, date of publication 6 February 2024, date of current version 12 February 2024.

Digital Object Identifier 10.1109/ACCESS.2024.3359421

RESEARCH ARTICLE

A Multi-Agent Model Based on Rooted Leadership Structure and General Dynamics and Self-Adaptive Mechanism

ZHIBIN ZENG, (Member, IEEE), ZILUO XIE, AND ZHENYU JIANG
School of Microelectronics, Xidian University, Xi'an 710071, China

Corresponding author: Zhibin Zeng (zbzeng@163.com)

This work was supported in part by Key Research and Development Program of Shaanxi, China, under Grant 2023-YBSF-147.

ABSTRACT This paper proposes a first-order multi-agent model that overcomes the limitations of previous models by incorporating rooted leadership structure, general nonlinear dynamics, and self-adaptive feedback mechanisms. The model consists of multiple agents positioned in a multidimensional space and a virtual leader with environmental perception. Each agent follows fixed general nonlinear dynamics, whereas the group's leadership structure follows an asymmetric fixed-coupling topology. The model is stable if certain mild assumptions about the agents' dynamics and group coupling topology are satisfied, as proven using the Lyapunov function method. In order to verify the effectiveness of this model in group outdoor motion, simulation results demonstrate that all agents ultimately dynamically form a cohesive swarm and follow the virtual leader's movement toward the destination, even in cases where the movements of all agents have a certain degree of randomness or in cases that the model scaled up to a much higher number of agents.

INDEX TERMS Multi-agent, nonlinear, rooted leadership, self-adaptive, stability.

I. INTRODUCTION

Individual movements interweaving and gathering together are pervasive in biological swarm activities. By modeling, simulating, and analyzing biological swarm activities, the demands of engineering applications such as multi-robot team formation control [1], [2], [3], pedestrian motion analysis and control [4], [5], [6], [7] can be met. Therefore, a large number of researchers were attracted to conduct research in the field of multi-agent systems. Several main control methods for multi-agent systems, such as leader-follower method [8], graph theory method [9], virtual potential field method [10], cooperative control method [11], and reinforcement learning method [12], have been developed.

The analysis of flocking is traced back to the relevant computer simulation work in [13], after which Gazi and Pasino designed a first-order multi-agent model consisting of several agents that can perceive environmental gradients in Euclidean space and the characteristics of flocking, consistency, and stability of the model were studied based on artificial potential field theory in [14] and [15]. In [16], Olfati-Saber proposed a theoretical framework for designing and analyzing distributed flocking algorithms, which solves the problems of unconstrained free flocking and flocking with obstacles. Furthermore, the stability and mill ring solutions of second-order multi-agent models were also studied in [17], [18], and [19]. In the study of Qin et al. [20], aiming at the second-order multi-agent system with clustering behavior, two hypotheses were established for the problem of the consistency constraint interval of agents in the system, which was studied from two aspects, namely, agents holding constraint interval independently and agents being affected by constraint interval of other agents. They proved the relationship between the constraint interval and the equilibrium point of the system by solving the nonlinear equations. They also proved the inevitable relationship between the equilibrium point and the system consistency by Lyapunov stability theory. Additionally, Liu et al. introduced the impact

The associate editor coordinating the review of this manuscript and approving it for publication was Laura Celentano.

of communication time delay into the multi-agent model in [21], and their research showed that flocking behavior occurs under certain conditions for asynchronous models with delay. However, the swarm will diverge when the time delay increases to a specific value. The research of Yang et al. [22] focuses on the distributed optimization problem of first-order multi-agent systems with time delay. The global objective function of the multi-agent system is assumed to be obtained by the superposition of local objective functions of each agent, and only the member corresponding to the local objective function knows its objective. Based on the above assumptions, they propose a distributed algorithm to optimize the state convergence problem among the agents and use the Lyapunov-Karasovsky method to prove the asymptotic consistency of the agent states, then illustrate the analysis results through a test example. Recently, Yuan et al. [23] focused on the clustering problem of a partially informed multi-agent system. They assumed that the receiving party of information was missing part of the information in the information transmission process. By introducing the Morse potential energy equation into the analysis of the clustering algorithm, the stability of the clustering algorithm was proved from two aspects: Lyapunov stability theory and the Lassalle invariance principle. Based on the above clustering algorithm, they also proposes an improved algorithm to add propagandists to the system, which can reduce the impact of information loss by making propagandists with all the information spread as agents. Simulation results show that such propagandists have a significant effect on ensuring system consistency. Besides, Das et al. introduced the chaos theory into the swarm model to analyze the chaotic phenomena in the swarm. Using the Lyapunov index, they studied the chaotic phenomena in the dimensionally separated social foraging swarms in [24]. To be precise, the conditions for chaos were analyzed, and the trajectories of agents in swarms with/without chaos were simulated. In [25], Das further analyzed the chaotic phenomena of dimensionally non-separable social foraging swarms. Moreover, Das proposed a new type of group dynamics that can be applied to automated multi-agent systems in [26], in which its stability and chaotic phenomena were studied. The results clarified how to control specific parameters to make the model exhibit different chaotic or non-chaotic behaviors.

However, the coupling topologies in the above models are globally symmetric, and it is well known that the coupling topology has specific influences on the model's behavior. So in [27] and [28], Liu et al. studied the stability and cohesion behavior of swarms with a generally invariant coupling topology, proving that swarms will exhibit flocking behavior and move towards more favorable environmental regions when the underlying coupling topology is strongly connected. Nevertheless, this leads to another issue, as it can be seen from [29] and [30] that there are often leader-follower structures in natural animal groups, so their coupling topologies generally do not meet the strongly connected requirements. To address this challenge, in [31], Shen proposed a model with a hierarchical leadership structure in which agents are only influenced by the upper level of their hierarchy. Various leadership structures have also been studied in papers such as [32], [33], [34], [35], [36], [37], and [38]. Recently, Li considered a swarm model in [39], where each agent has general inherent nonlinear dynamics and the interactions between agents adhere to a rooted leadership topology, which means that there exists an overall leader directly or indirectly leads any other agent (Fig.1 shows a multi-agent system's rooted and unrooted leadership topology containing only two agents). It is proved that the swarm remains both stable and cohesive when the symmetric matrix derived from the group coupling topology is negative definite.

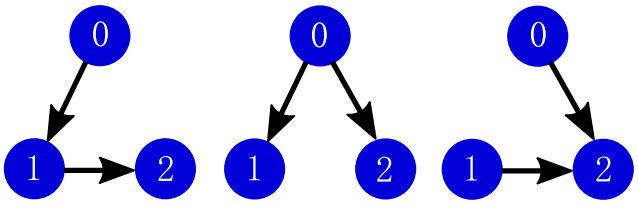

FIGURE 1. The left and middle parts show two rooted leadership topologies while the right part demonstrate an unrooted leadership as there is no direct or indirect leadership path from the overall leader (agent 0) to agent 1.

Most of the above papers assume that the attraction between agents increases linearly with their relative distance and that the attraction/repulsion functions between agents always include a linear attraction term. To be more precisely, the attraction/repulsion functions between each two agents can be described in the following form:

$$g(y) = y\left(g_a(\|y\|) - g_r(\|y\|)\right),$$

where y is the vector that reflects the relative position between two agents, and at the same time, $g_a(\|y\|)\,y$ and $g_r(\|y\|)\,y$ represent the attractive and repulsive force between agents, respectively. However, both were often assumed to take certain forms like $g_a(\|y\|) = a$ and $g_r(\|y\|) = -b\exp\left(-\frac{\|y\|^2}{c}\right)$, where a, b, and c are positive constants [14], [15], [27], [28], [40]. This overly strong assumption about attraction/repulsion functions results in a limited scope of application of the model, as it excludes many scenarios that have the potential to be applied to first-order multi-agent systems, for instance, the attraction (gravitational force) between moving celestial bodies is inversely proportional to the square of the distance between them, rather than linearly varying with the distance. Another reason for relaxing the assumptions is that the leadership structure and the attraction/repulsion functions between agents are intrinsic factors that cannot be externally controlled and usually have some randomness in real-life scenarios such as group motions in outdoor environments, which means even if the approximate range of attraction/repulsion functions are certain, accurately fit their expressions is still impossible. Therefore, further relaxing the assumptions and abstracting

the attraction/repulsion functions are crucial for improving the generality of the model to apply to more practical scenarios. Though the swarm model recently considered by Li in [39] no longer assumes the specific form of $g_a(\|y\|)$, it still supposes $g_a(\|y\|)\|y\| \leq b$ and retains $g_a(\|y\|) = a$. To address this challenge, this paper proposes a first-order multi-agent model that incorporates a rooted leadership structure and a nonspecific inter-agent attraction/repulsion function and uses the self-adaptive feedback mechanisms of the virtual leader to enhance the cohesion of the group further. Under mild assumptions, when the undirected coupling topology of all members has connectivity, the stability of the model was proved by using Lyapunov function methods. The simulation results demonstrate that, with a certain degree of randomness of movements, agents still gather around the virtual leader for a finite time and follow its movement, which indicates that the proposed model is well-suited for outdoor group motion applications.

The rest of this paper is organized as follows. Section II introduces a multi-agent model with a rooted leadership, general nonlinear dynamics structure, and the virtual leader's self-adaptive feedback mechanisms. Section III, a specific boundary to which the population size converges, was derived based on certain assumptions, and the convergence time was estimated. The computational complexity of the model and the influence of some parameters in the model on the performance were analyzed. In Section IV, numerical simulation experiments were provided to validate the theory. The conclusion is presented in Section V.

II. MULTI-AGENT MODEL

This section proposes a multi-agent model with general nonlinear dynamics and rooted leadership. A m-dimensional space, which includes n agents and a virtual leader who has direct leadership over these n agents, was considered in this model. For simplifying this model, the leader and all agents are considered particles. At any moment, there exists a pair of relative velocity vectors in opposite directions between any two agents of the model. Moreover, the norm of this pair of vectors is determined by the magnitude of the relative distance and the two fixed weights between agents at the current moment. Thus, for any agent of the model, the actual velocity vector at each moment is a weighted linear superposition of the current moment's relative velocity vectors with all other members and with the virtual leader. This relationship is expressed as the following equation of motion:

$$\dot{x}_i = \sum_{j=0, j\neq i}^{n} w_{ij} g\left(x_j - x_i\right), \quad i = 1, 2, \ldots, n, \tag{1}$$

where $g : R^m \to R^m$denotes the relationship between the relative velocity and relative position vector between the two agents, and the non-negative constant w_{ij} denotes the fixed weight of the relative velocity component affected by agent j when calculating the actual velocity for agent i. Therefore, a $n+1$ dimensional matrix $W = \left[w_{ij}\right]_{(n+1)\times(n+1)}$ is defined to reflect the rooted leadership structure of the entire group, including all agents and the virtual leader, where w_{ij} is the element in the ith row and jth column, and $w_{ij} > 0$ only if the motion of agent i is affected by agent i, otherwise, $w_{ij} = 0$.

Since only the virtual leader can perceive environmental information, it is responsible for utilizing the external navigation data it perceives, as well as its influence on the movement of all agents, to gather all agents into its boundaries and guide them to their destination. Therefore, the motion of the virtual leader should not directly depend on the coordinates of any agents, which means $w_{0j} = 0$ for any $j = 1, 2, \ldots, n$. Up to this point, it is shown that the first row and diagonal elements of W are all 0. At the same time, the rooted leadership property guarantees that the number of positive elements in the first column is not less than the number of connected components of the swarm, because there needs at least one directly lead force for each connected component to make the rooted leadership property possible. The rest of the elements are non-negative. Thus, W has the following form:

$$W = \begin{pmatrix} 0 & 0 & 0 & \cdots & \cdots & 0 \\ w_{10} & 0 & w_{12} & \cdots & \cdots & w_{1n} \\ w_{20} & w_{21} & 0 & & & w_{2n} \\ \vdots & \vdots & & \ddots & & \vdots \\ \vdots & \vdots & & & \ddots & \vdots \\ w_{n0} & w_{n1} & w_{n2} & \cdots & \cdots & w_{nn} \end{pmatrix}$$

However, to enhance the cohesion of the group, the speed of the virtual leader is partly adjusted by the feedback from the real-time cohesion degree of the group. To be more precise, the virtual leader will increase its speed to lead the swarm forward faster when most agents have firmly clustered around it. In the absence of cohesion, however, the virtual leader prioritizes gathering all agents within their boundaries rather than moving forward as fast as possible. Then, the motion equation of the virtual leader can be expressed as follows:

$$\dot{x}_0 = \frac{f(x_0)}{\frac{1}{n}\sum_{i=1}^{n}\|x_i - x_0\|}, \tag{2}$$

where $f : R^m \to R^m$ denotes the external influences on the leader's velocity, and the denominator of (2) denotes the feedback from the swarm's cohesion. Due to the repulsion between agents and the leader, it is ensured that $\|x_i - x_0\| > 0$ for any agent at any time unless the initial position of the agent overlaps with the leader.

Moreover, it is well known that in many practical application scenarios of multi-agent models, including outdoor group motion, the positions of the agents never overlap, which leads to an implicit condition that the mapping function g for the m-dimensional vector can be expressed as $g(y) = \frac{\mu(\|y\|)}{\|y\|}y$, where $\mu : R^+ \to R$, $\|y\| > 0$, $\lim_{\|y\|\to 0}\mu(\|y\|) = -\infty$.

Therefore, the motion equation system is rewritten as follows:

$$\dot{x}_0 = \frac{f(x_0)}{\frac{1}{n}\sum_{i=1}^{n}\|x_i - x_0\|}.$$
$$\dot{x}_i = \sum_{j=0, j\neq i}^{n} w_{ij}\frac{\mu\left(\left\|x_j - x_i\right\|\right)}{\left\|x_j - x_i\right\|}\left(x_j - x_i\right), \quad i = 1, 2, \ldots, n. \tag{3}$$

III. MODEL STABLITY ANALYSIS

A. CONVERGENCE ANALYSIS

In this section, the stability of the multi-agent model described in (3) in terms of its cohesiveness was studied. To accomplish this, the variable $e_i = x_i - x_0$ was first defined to portray the relative positional relationship between agent i and the virtual leader. Then, In order to analyze the state of the multi-agent system, a suitable Lyapunov function that reflects the overall size of the swarm is constructed as follows:

$$V(e) = \frac{1}{2}\|e\|^2 = \frac{1}{2}\sum_{i=1}^{n}\|e_i\|^2 = \frac{1}{2}\sum_{i=1}^{n} e_i^T e_i, \tag{4}$$

where $e = \left(e_1^T, e_2^T, \ldots, e_n^T\right)^T$ is a nm-dimensional column vector. Then, from the equations of motion in (3), the expression for the derivative of e_i concerning time can be derived as follows:

$$\begin{aligned}\dot{e}_i &= \dot{x}_i - \dot{x}_0 \\ &= -\frac{nf(x_0)}{\sum_{i=1}^{n}\|e_i\|} + w_{i0}\frac{\mu(\|x_0 - x_i\|)}{\|x_0 - x_i\|}(x_0 - x_i) \\ &\quad + \sum_{j=1}^{n} w_{ij}\frac{\mu\left(\left\|x_j - x_i\right\|\right)}{\left\|x_j - x_i\right\|}\left(x_j - x_i\right) \\ &= -\frac{nf(x_0)}{\sum_{i=1}^{n}\|e_i\|} - w_{i0}\frac{\mu(\|e_i\|)}{\|e_i\|}e_i \\ &\quad + \sum_{j=1}^{n} w_{ij}\frac{\mu\left(\left\|e_j - e_i\right\|\right)}{\left\|e_j - e_i\right\|}\left(e_j - e_i\right), \quad i = 1, 2, \ldots, n.\end{aligned} \tag{5}$$

According to the previous discussion, firstly, the attraction/repulsion between agents follows near-repulsion and far-attraction. However, the function of the attraction/repulsion does not have a specific form that necessarily has a linear component. Secondly, when the initial positions of each agent do not overlap, it is clear that there exists $r_{\min} > 0$ such that the distance of any agent at any time t satisfies $\left\|x_j - x_i\right\| \geq r_{\min}$, which means that μ has a lower bound. Thirdly, f is an external navigation input from the environment that is adjusted by the currunt cohesion degree of the swarm. Finally, the coupling topology of the swarm, which is embodied in matrix W, has specific influences on the model's behavior. Therefore, the following three assumptions are made about f, μ and W.

Assumption 1: For all $x \in R^m$, there exists a positive constant θ such that $\|f(x)\| \leq \theta$, which is the bound of external inputs on the leader in (2).

Assumption 2: The continuous function μ in (3) exists a unique zero point $r_0 > 0$ and a minimum distance $0 < r_{\min} < r_0$ for any pair of agents during all time. Suppose the distance between agents is $\|y\|$, then μ satisfies $\mu(\|y\|) > 0$ when $\|y\| > r_0$, $-\underline{M} \leq \mu(\|y\|) < 0$ when $r_{\min} \leq \|y\| < r_0$, where M is a positive constant.

Assumption 3: The matrix $(W + W^T)$ has connectivity during all the time. This means a direct or indirect relationship always exists between any two agents after all the directed edges representing the leadership relationship in matrix W are transformed into undirected edges.

1) CONVERGENCE SIZE ESTIMATED

By utilizing the Lyapunov function constructed in (4), the following theorem is derived.

Theorem 1: Considering the multi-agent system described in (3), given arbitrary initial positions where all agents do not coincide, then all agents will eventually enter into a bounded region around the leader under the conditions of **Assumptions 1, 2, and 3**, which means $V(e(t)) \to \gamma^2$ when $t \to \infty$, where $\gamma = \frac{\sqrt{n}\beta\overline{d} + \sqrt{n\beta^2\overline{d}^2 + (2\delta r_0 n\overline{\lambda} + 4n\theta)\left(\underline{v}\underline{d} + \alpha\lambda_2\left(1 - \frac{m}{n}\right)\right)}}{2\left(\underline{v}\underline{d} + \alpha\lambda_2\left(1 - \frac{m}{n}\right)\right)}$, m, n, r_0, θ have the meanings mentioned earlier, whereas β, α, $\overline{d}$, $\underline{d}$, $\overline{\lambda}$, λ_2 are parameters related to W, f, μ.

Proof: According to (4) and (5), the derivative of function $V(e(t))$ with time t is represented as follows:

$$\begin{aligned}\dot{V}(e) &= \frac{1}{2}\sum_{i=1}^{n}\left(e_i^T\dot{e}_i + \dot{e}_i^T e_i\right) = \sum_{i=1}^{n} e_i^T\dot{e}_i \\ &= \sum_{i=1}^{n} e_i^T\left\{-\frac{nf(x_0)}{\sum_{i=1}^{n}\|e_i\|} - w_{i0}\frac{\mu(\|e_i\|)}{\|e_i\|}e_i\right\} \\ &\quad + \sum_{i=1}^{n} e_i^T\sum_{j=1}^{n} w_{ij}\frac{\mu\left(\left\|e_j - e_i\right\|\right)}{\left\|e_j - e_i\right\|}\left(e_j - e_i\right).\end{aligned} \tag{6}$$

For the first term of (6), the following can be inferred from the **Assumption 1** and (2).

$$\begin{aligned}\sum_{i=1}^{n} e_i^T\left\{-\frac{nf(x_0)}{\sum_{i=1}^{n}\|e_i\|}\right\} &\leq \frac{\left\|\sum_{i=1}^{n} e_i^T\right\|}{\sum_{i=1}^{n}\|e_i\|}\|-nf(x_0)\| \\ &\leq \frac{\sum_{i=1}^{n}\|e_i\|}{\sum_{i=1}^{n}\|e_i\|}n\|f(x_0)\| \leq n\theta.\end{aligned} \tag{7}$$

Since **Assumption 2** is satisfied, the following two sets are defined to delineate the agents that lie within and outside the attraction/repulsion equilibrium distance of the virtual leader.

$$A_1 := \{i \,|\, i = 1, 2, \ldots, n\ , \|e_i\| \le r_0, w_{i0} > 0\}\,.$$
$$A_2 := \{i \,|\, i = 1, 2, \ldots, n\ , \|e_i\| > r_0, w_{i0} > 0\}\,.$$

Then for the second term of (6), there is

$$\begin{aligned}
&-\sum_{i=1}^{n} w_{i0} e_i^T \frac{\mu\left(\|e_i\|\right)}{\|e_i\|} e_i \\
&= -\sum_{i\in A_1} w_{i0} e_i^T \frac{\mu\left(\|e_i\|\right)}{\|e_i\|} e_i - \sum_{i\in A_2} w_{i0} e_i^T \frac{\mu\left(\|e_i\|\right)}{\|e_i\|} e_i \\
&= -\sum_{i\in A_1} w_{i0} e_i^T \frac{\underline{M}}{\|e_i\|} e_i - \sum_{i\in A_2} w_{i0} e_i^T \frac{\mu\left(\|e_i\|\right)}{\|e_i\|} e_i \\
&\quad - \sum_{i\in A_1} w_{i0} e_i^T \left(\frac{\mu\left(\|e_i\|\right) - \underline{M}\,\|e_i\|}{\|e_i\|}\right) e_i. \qquad (8)
\end{aligned}$$

Define $v := \min_{\{i\in A_2\}} \left(\underline{M}, \frac{\mu(\|e_i\|)}{\|e_i\|}\right) \ge 0$ ($v = 0$ if and only if A_2 is an empty set) to merge the first and third terms of (8) to obtain the following form:

$$\begin{aligned}
-\sum_{i=1}^{n} w_{i0} e_i^T \frac{\mu\left(\|e_i\|\right)}{\|e_i\|} e_i &\le \sum_{i\in A_1} w_{i0} e_i^T \left(\frac{-\mu\left(\|e_i\|\right) + \underline{M}\,\|e_i\|}{\|e_i\|}\right) e_i \\
&\quad - v \sum_{i=1}^{n} w_{i0} e_i^T e_i. \qquad (9)
\end{aligned}$$

Define $\beta := \max_{\{i\in A_1\}} \left(-\mu\left(\|e_i\|\right) + \underline{M}\,\|e_i\|\right) \ge 0$ ($\beta = 0$ if and only if A_1 is an empty set) to further reduce (9) to inequality below.

$$-\sum_{i=1}^{n} w_{i0} e_i^T \frac{\mu\left(\|e_i\|\right)}{\|e_i\|} e_i \le -v \sum_{i=1}^{n} w_{i0} e_i^T e_i + \beta \sum_{i\in A_1} \frac{w_{i0}}{\|e_i\|} e_i^T e_i. \qquad (10)$$

Define $\overline{d} := \max_{\{i=1,2,\ldots,n\}} (w_{i0}) \ge 0$ and $\underline{d} := \min_{\{i=1,2,\ldots,n\}} (w_{i0}) \ge 0$, which denote the maximum/minimum weights of the virtual leader's impact on all agents, respectively, and this leads to the further deflation of (10) as follows:

$$\begin{aligned}
-\sum_{i=1}^{n} w_{i0} e_i^T \frac{\mu\left(\|e_i\|\right)}{\|e_i\|} e_i &\le -v\underline{d} \sum_{i=1}^{n} e_i^T e_i + \beta\overline{d} \sum_{i\in A_1} e_i^T \frac{e_i}{\|e_i\|} \\
&\le -2v\underline{d} V\,(e) + \beta\overline{d} \sum_{i=1}^{n} e_i^T \frac{e_i}{\|e_i\|}. \qquad (11)
\end{aligned}$$

Then, by using the mean inequality

$$\sum_{i=1}^{n} e_i^T \frac{e_i}{\|e_i\|} \le \sqrt{n \sum_{i=1}^{n} e_i^T e_i} = \sqrt{2nV\,(e)}$$

in (11), the final form of the second term of (6) is obtained as follows:

$$-\sum_{i=1}^{n} w_{i0} e_i^T \frac{\mu\left(\|e_i\|\right)}{\|e_i\|} e_i \le -2v\underline{d} V\,(e) + \beta\overline{d}\sqrt{2nV\,(e)}. \qquad (12)$$

Now, as for the third term of (6), it conforms to the following transformation:

$$\begin{aligned}
&\sum_{i=1}^{n} e_i^T \sum_{j=1}^{n} w_{ij} \frac{\mu\left(\|e_j - e_i\|\right)}{\|e_j - e_i\|} \left(e_j - e_i\right) \\
&= \sum_{i=1}^{n} \sum_{j=1}^{n} w_{ij} e_i^T \frac{\mu\left(\|e_j - e_i\|\right)}{\|e_j - e_i\|} \left(e_j - e_i\right) \\
&= \frac{1}{2} \sum_{i=1}^{n} \sum_{j=1}^{n} w_{ij} e_i^T \frac{\mu\left(\|e_j - e_i\|\right)}{\|e_j - e_i\|} \left(e_j - e_i\right) \\
&\quad + \frac{1}{2} \sum_{i=1}^{n} \sum_{j=1}^{n} w_{ji} e_j^T \frac{\mu\left(\|e_j - e_i\|\right)}{\|e_j - e_i\|} \left(e_i - e_j\right) \\
&= -\frac{1}{2} \sum_{i=1}^{n} \sum_{j=1}^{n} \left(w_{ij} + w_{ji}\right) \left(e_j - e_i\right)^T \frac{\mu\left(\|e_j - e_i\|\right)}{\|e_j - e_i\|} \left(e_j - e_i\right). \qquad (13)
\end{aligned}$$

The subsequent treatment is similar to the second term of (6). Two sets are defined below to delineate pairs of agents that are within and outside the equilibrium distance of their attraction/repulsion.

$$\begin{aligned}
&A_3 \\
&:= \left\{(i,j)\ |i,j \in \{1,2,\ldots n\}\ , \left\|e_i - e_j\right\| \le r_0, w_{ij} + w_{ji} > 0\right\}. \\
&A_4 \\
&:= \left\{(i,j)\ |i,j \in \{1,2,\ldots n\}\ , \left\|e_i - e_j\right\| > r_0, w_{ij} + w_{ji} > 0\right\}.
\end{aligned}$$

So (13) is transformed into

$$\begin{aligned}
&\sum_{i=1}^{n} e_i^T \left\{\sum_{j=1}^{n} w_{ij} \frac{\mu\left(\|e_j - e_i\|\right)}{\|e_j - e_i\|} \left(e_j - e_i\right)\right\} \\
&= -\frac{1}{2} \sum_{(i,j)\in A_3} \left(w_{ij} + w_{ji}\right) \left(e_j - e_i\right)^T \frac{\mu\left(\|e_j - e_i\|\right)}{\|e_j - e_i\|} \left(e_j - e_i\right) \\
&\quad - \frac{1}{2} \sum_{(i,j)\in A_4} \left(w_{ij} + w_{ji}\right) \left(e_j - e_i\right)^T \frac{\mu\left(\|e_j - e_i\|\right)}{\|e_j - e_i\|} \left(e_j - e_i\right) \\
&= -\frac{1}{2} \sum_{(i,j)\in A_4} \left(w_{ij} + w_{ji}\right) \left(e_j - e_i\right)^T \frac{\mu\left(\|e_j - e_i\|\right)}{\|e_j - e_i\|} \left(e_j - e_i\right) \\
&\quad - \frac{1}{2} \sum_{(i,j)\in A_3} \left(w_{ij} + w_{ji}\right) \left(e_j - e_i\right)^T \underline{M} \left(e_j - e_i\right) \\
&\quad - \frac{1}{2} \sum_{(i,j)\in A_3} \left\{\frac{\mu\left(\|e_j - e_i\|\right) - \underline{M}\,\|e_j - e_i\|}{\|e_j - e_i\|}\right. \\
&\quad \left. \times \left(w_{ij} + w_{ji}\right) \left(e_j - e_i\right)^T \left(e_j - e_i\right)\right\}. \qquad (14)
\end{aligned}$$

Furtherly, define $\alpha := \min_{\{(i,j)\in A_4\}}\left(\underline{M}, \frac{\mu(\|e_i-e_j\|)}{\|e_i-e_j\|}\right) \geq 0$ ($\alpha = 0$ if and only if A_4 is an empty set) and $\delta := \max_{\{(i,j)\in A_3\}}\left(-\mu\left(\|e_i-e_j\|\right)+\underline{M}\|e_i-e_j\|\right) \geq 0$ ($\delta = 0$ if and only if A_3 is an empty set), thus (14) can further written as

$$\begin{aligned}
&\sum_{i=1}^{n} e_i^T \sum_{j=1}^{n} w_{ij}\frac{\mu\left(\|e_j-e_i\|\right)}{\|e_j-e_i\|}\left(e_j-e_i\right)\\
&\leq -\frac{1}{2}\alpha\sum_{i=1}^{n}\sum_{j=1}^{n}\left(w_{ij}+w_{ji}\right)\left(e_j-e_i\right)^T\left(e_j-e_i\right)\\
&\quad+\frac{1}{2}\sum_{(i,j)\in A_3}\left\{\frac{-\mu\left(\|e_j-e_i\|\right)+\underline{M}\|e_j-e_i\|}{\|e_j-e_i\|}\right.\\
&\left.\times\left(w_{ij}+w_{ji}\right)\left(e_j-e_i\right)^T\left(e_j-e_i\right)\right\}\\
&\leq -\frac{1}{2}\alpha\sum_{i=1}^{n}\sum_{j=1}^{n}\left(w_{ij}+w_{ji}\right)\left(e_j-e_i\right)^T\left(e_j-e_i\right)\\
&\quad+\frac{1}{2}\sum_{(i,j)\in A_3}\left(w_{ij}+w_{ji}\right)\left(e_j-e_i\right)^T\frac{\delta}{\|e_j-e_i\|}\left(e_j-e_i\right)\\
&= -\frac{1}{2}\alpha\sum_{i=1}^{n}\sum_{j=1}^{n}\left(w_{ij}+w_{ji}\right)\left(e_j-e_i\right)^T\left(e_j-e_i\right)\\
&\quad+\frac{1}{2}\delta\|e_j-e_i\|\sum_{(i,j)\in A_3}\left(w_{ij}+w_{ji}\right)\frac{\left(e_j-e_i\right)^T}{\|e_j-e_i\|}\frac{\left(e_j-e_i\right)}{\|e_j-e_i\|}\\
&\leq -\frac{1}{2}\alpha\sum_{i=1}^{n}\sum_{j=1}^{n}\left(w_{ij}+w_{ji}\right)\left(e_j-e_i\right)^T\left(e_j-e_i\right)\\
&\quad+\frac{1}{2}\delta r_0\sum_{(i,j)\in A_3}\left(w_{ij}+w_{ji}\right)\\
&\leq -\frac{1}{2}\alpha\sum_{i=1}^{n}\sum_{j=1}^{n}\left(w_{ij}+w_{ji}\right)\left(e_j-e_i\right)^T\left(e_j-e_i\right)\\
&\quad+\frac{1}{2}\delta r_0\sum_{i=1}^{n}\sum_{j=1}^{n}\left(w_{ij}+w_{ji}\right).
\end{aligned}\tag{15}$$

For further treatment of (15), define symmetric matrix $Y = \left[y_{ij}\right]_{n\times n}$, where $y_{ij} = w_{ij}+w_{ji}$, and the Laplacian of matrix Y is denoted by $L = \left[l_{ij}\right]_{n\times n}$, where

$$l_{ij} = \begin{cases} -y_{ij}, & i\neq j\\ \sum_{j=1,j\neq i}^{n} y_{ij}, & i=j \end{cases}\tag{16}$$

By the definition of Laplacian L of coupling matrix, it is deduced that the second term of (15) can turns into

$$\begin{aligned}
&\frac{1}{2}\delta r_0\sum_{i=1}^{n}\sum_{j=1}^{n}\left(w_{ij}+w_{ji}\right)\\
&=\frac{1}{2}\delta r_0\sum_{i=1}^{n}\sum_{j=1}^{n}y_{ij}\\
&=\frac{1}{2}\delta r_0\sum_{i=1}^{n}l_{ii}=\frac{1}{2}\delta r_0 Tr\left(L\right)=\frac{1}{2}\delta r_0 n\bar{\lambda}>0,
\end{aligned}\tag{17}$$

where Tr represents the trace of the matrix, and $\bar{\lambda} = \frac{1}{n}\sum_{i=1}^{n}\lambda_i > 0$ is the arithmetic mean of all eigenvalues of L.

Meanwhile, the first item of (15) is treated as follows

$$\begin{aligned}
&-\frac{1}{2}\alpha\sum_{i=1}^{n}\sum_{j=1}^{n}\left(w_{ij}+w_{ji}\right)\left(e_j-e_i\right)^T\left(e_j-e_i\right)\\
&=-\frac{1}{2}\alpha\sum_{i=1}^{n}\sum_{j=1}^{n}y_{ij}\left(e_j^Te_j+e_i^Te_i-e_j^Te_i-e_i^Te_j\right)\\
&=-\frac{1}{2}\alpha\left(\sum_{j=1}^{n}e_j^Te_j\sum_{i=1}^{n}y_{ij}+\sum_{i=1}^{n}e_i^Te_i\sum_{j=1}^{n}y_{ij}\right)\\
&\quad+\alpha\sum_{i=1}^{n}\sum_{j=1}^{n}y_{ij}e_i^Te_j\\
&=-\alpha\left(\sum_{i=1}^{n}l_{ii}e_i^Te_i-\sum_{i=1}^{n}\sum_{j=1,j\neq i}^{n}y_{ij}e_i^Te_j\right)\\
&=-\alpha\left(\sum_{i=1}^{n}l_{ii}e_i^Te_i+\sum_{i=1}^{n}\sum_{j=1,j\neq i}^{n}l_{ij}e_i^Te_j\right)\\
&=-\alpha\sum_{i=1}^{n}\sum_{j=1}^{n}l_{ij}e_i^Te_j=e^T\left(L\otimes I_m\right)e.
\end{aligned}\tag{18}$$

Note that the real symmetric matrix L corresponds to a unique orthogonal matrix P satisfying $P^TLP = \Lambda$, where Λ is a diagonal matrix with elements on the main diagonal from λ_1 to λ_n. And [41] proved that all eigenvalues of the Laplacian matrix of n-th order symmetric matrix with connectivity like Y satisfy $0 = \lambda_1 < \lambda_2 \leq \ldots\ldots \leq \lambda_n$. So after presuming that $e^T\left(P\otimes I_m\right) = \left(c_1, c_2, \ldots c_{m\times n}\right)$, there is

$$\begin{aligned}
&e^T\left(L\otimes I_m\right)e\\
&=e^T\left(P\otimes I_m\right)\left(\Lambda\otimes I_m\right)\left(P\otimes I_m\right)^Te\\
&=\lambda_1\sum_{i=1}^{m}c_i^2+\lambda_2\sum_{i=m+1}^{2m}c_i^2+\ldots+\lambda_n\sum_{i=m(n-1)+1}^{mn}c_i^2\\
&=\lambda_2\sum_{i=m+1}^{2m}c_i^2+\ldots+\lambda_n\sum_{i=m(n-1)+1}^{mn}c_i^2.
\end{aligned}\tag{19}$$

Since the elements of each row of L sum to 0, the first column of P is the only linearly independent eigenvector p_1 corresponding to the single eigenvalue $\lambda_1 = 0$ of L, which means all elements in p_1 are $\frac{1}{\sqrt{n}}$, and the form of the first m

columns of $P \otimes I_m$ are as follows:

$$Q_{mn\times m} = (P \otimes I_m)(:, 1:m) = \begin{pmatrix} \frac{1}{\sqrt{n}} & & \\ & \ddots & \\ & & \frac{1}{\sqrt{n}} \\ \vdots & \vdots & \vdots \\ \frac{1}{\sqrt{n}} & & \\ & \ddots & \\ & & \frac{1}{\sqrt{n}} \end{pmatrix} \tag{20}$$

Therefore

$$\sum_{i=1}^{m} c_i^2 = e^T Q Q^T e = \left(\frac{1}{\sqrt{n}}\sum_{i=1}^{n} e_i\right)^T \left(\frac{1}{\sqrt{n}}\sum_{i=1}^{n} e_i\right) = \frac{1}{n}\left\|\sum_{i=1}^{n} e_i\right\|^2. \tag{21}$$

Substituting (21) into (19) yields

$$\begin{aligned} & e^T (L \otimes I_m) e \\ &= \lambda_2 \sum_{i=m+1}^{2m} c_i^2 + \ldots + \lambda_n \sum_{i=m(n-1)+1}^{mn} c_i^2 \\ &\geq \lambda_2 \sum_{i=m+1}^{mn} c_i^2 = \lambda_2 \left(\sum_{i=1}^{mn} c_i^2 - \sum_{i=1}^{m} c_i^2\right) \\ &= \lambda_2 \left(\|e\|^2 - \frac{1}{n}\left\|\sum_{i=1}^{n} e_i\right\|^2\right) \\ &= \lambda_2 \left(\|e\|^2 - \frac{1}{n}\sum_{i=1}^{n}\left(\sum_{j=1}^{m} e_{i:j}\right)^2\right) \\ &\geq \lambda_2 \left(\|e\|^2 - \frac{1}{n}\sum_{i=1}^{n} m \sum_{j=1}^{m} e_{i:j}^2\right) \\ &= \lambda_2 \left(\|e\|^2 - \frac{m}{n}\sum_{i=1}^{n}\sum_{j=1}^{m} e_{i:j}^2\right) = \lambda_2 \left(1 - \frac{m}{n}\right)\|e\|^2, \end{aligned} \tag{22}$$

where $e_{i:j}$ is the jth element of e_i. Obviously, $m \ll n$ in practical application scenarios, so

$$\begin{aligned} e^T (L \otimes I_m) e &\geq \lambda_2 \left(1 - \frac{m}{n}\right)\|e\|^2 \\ &= 2\lambda_2 \left(1 - \frac{m}{n}\right) V(e) > 0. \end{aligned} \tag{23}$$

Then the final scaling result of (6) was obtained below by comprehensively considering (7), (12), (17), (23).

$$\begin{aligned} \dot{V}(e) \leq & -\left(v\underline{d} + \alpha\lambda_2\left(1 - \frac{m}{n}\right)\right) 2V(e) \\ & + \sqrt{n}\beta\overline{d}\sqrt{2V(e)} + \frac{1}{2}\delta r_0 n\bar{\lambda} + n\theta. \end{aligned} \tag{24}$$

Thus the sufficient condition for $\dot{V}(e) < 0$ to be derived by (24) is

$$\begin{aligned} & \|e\| > \gamma \\ &= \frac{\sqrt{n}\beta\overline{d} + \sqrt{n\beta^2\overline{d}^2 + n\left(2\delta r_0\bar{\lambda} + 4\theta\right)\left(v\underline{d} + \alpha\lambda_2\left(1 - \frac{m}{n}\right)\right)}}{2\left(v\underline{d} + \alpha\lambda_2\left(1 - \frac{m}{n}\right)\right)}. \end{aligned} \tag{25}$$

That means all agents will eventually converge to a bounded area within a specific range near the leader, as shown in **Theorem 1**. It should be noted that due to the widespread use of the scaling method in various assumptions and proofs presented in this section, the result of **Theorem 1** is a very conservative estimate, so the actual size that the entire swarm converges to should be less than γ. Moreover, the proof of **Theorem 1** fails if both v and α are 0 (theoretically possible) because the denominator of γ is 0. However, the occurrence of this situation means that the distance between any pair of agents (including the overall leader) is less than the equilibrium distance of the repulsive/attractive force. That is, only the repulsive force exists between agents, which means that the swarm has converged to an extremely tight state that is impossible to stabilize and must diverge back to the actual steady state. Therefore, this paper will only consider the discussion without this situation.

2) CONVERGENCE TIME ESTIMATED

Furthermore, the convergence time can also be estimated from (24).

Theorem 2: Consider the converged $V(e)$ estimated in **Theorem 1**. for any $\rho_1 > \rho_2 > \frac{1}{2}\gamma_1^2$, the time required for $V(e)$ to converge from ρ_1 to ρ_2 will not exceed $k(\rho_1, \rho_2) = h(\rho_1) - h(\rho_2)$, where

$$\begin{aligned} h(\rho) = & \frac{1}{2\sqrt{\Delta}}\left\{\gamma_1 \ln\left(\sqrt{2\rho} - \gamma_1\right) - \gamma_2 \ln\left(\sqrt{2\rho} - \gamma_2\right)\right\}, \\ & \rho > \frac{1}{2}\gamma_1^2. \end{aligned} \tag{26}$$

$$\Delta = \frac{1}{4}n\beta^2\overline{d}^2 + \left(\frac{1}{2}\delta r_0 n\bar{\lambda} + n\theta\right)\left(v\underline{d} + \alpha\lambda_2\left(1 - \frac{m}{n}\right)\right). \tag{27}$$

$$\gamma_1 = \gamma = \frac{\frac{1}{2}\sqrt{n}\beta\overline{d} + \sqrt{\Delta}}{v\underline{d} + \alpha\lambda_2\left(1 - \frac{m}{n}\right)} > 0. \tag{28}$$

$$\gamma_2 = \frac{\frac{1}{2}\sqrt{n}\beta\overline{d} - \sqrt{\Delta}}{v\underline{d} + \alpha\lambda_2\left(1 - \frac{m}{n}\right)} < 0. \tag{29}$$

Proof: The following derivation from (24) is a simple way to obtain an estimate of convergence time of $V(e)$

$$\begin{aligned}
&\frac{d\left(V\left(e\right)\right)}{dt}\\
&\leq -\left(v\underline{d}+\alpha\lambda_2\left(1-\frac{m}{n}\right)\right)\left(\sqrt{2V\left(e\right)}-\gamma_1\right)\\
&\quad\times\left(\sqrt{2V\left(e\right)}-\gamma_2\right).\\
&\int_{T_1}^{T_2}dt\\
&\leq -\frac{\int_{V(e(T_1))}^{V(e(T_2))}\left(\frac{1}{\sqrt{2V(e)}-\gamma_1}-\frac{1}{\sqrt{2V(e)}-\gamma_2}\right)d\left(V\left(e\right)\right)}{\left(v\underline{d}+\alpha\lambda_2\left(1-\frac{m}{n}\right)\right)\left(\gamma_1-\gamma_2\right)}.\\
&T\\
&\leq -\frac{\left\{\gamma_1\ln\left(\sqrt{2V\left(e\right)}-\gamma_1\right)-\gamma_2\ln\left(\sqrt{2V\left(e\right)}-\gamma_2\right)\right\}\Big|_{V(e(T_1))}^{V(e(T_2))}}{2\sqrt{\Delta}}\\
&=h\left(e\left(T_1\right)\right)-h\left(e\left(T_2\right)\right)=k\left(e\left(T_1\right),e\left(T_2\right)\right).
\end{aligned}\tag{30}$$

B. COMPUTATIONAL COMPLEXITY ANALYSIS

After the estimated convergence size and time were obtained at (25) and (30), respectively, analyzing their computational complexity is beneficial for evaluating the scalability and practicality of the model. A straightforward method to achieve this involves analyzing the time and space complexity needed to compute each parameter in their expression. Since m, n, and r_0 are the dimension of the space, the number of agents, and the unique zero point of attractive/repulsive function μ, respectively, their time and space complexity are both $O(1)$; θ is the upper bound on the modulus of the virtual leader's motion equation f, which is a m-dimensional vector. Therefore, the space and time complexity of θ equals $O(m)$; $\overline{d}$ and $\underline{d}$ are the maximum and minimum values of the n elements in the first column (except the first element w_{00}) of the topology matrix W, respectively. Thus, their space and time complexity are $O(1)$ and $O(n)$, respectively; Review the definitions of the four parameters β, v, δ, and α in the previous part of this section. It is evident that their values change over time, and the computations of β and v at each moment need calculating all n modulus of m-dimensional vectors $\|e_i\|$ first, while δ and α need calculating $n(n-1)/2$ modulus of m-dimensional vectors since their parameters are $\|e_i-e_j\|$ rather than $\|e_i\|$. Therefore, the time complexity of β and v are both $O(mn)$, while δ and α are both $O(mn^2)$. And the space complexities of all these four parameters are $O(1)$; As for $\overline{\lambda}$ and λ_2, they are the most computationally intensive since the calculation of matrix eigenvalues was involved. According to (16), time and space complexity for computing and storing all elements of the Laplacian matrix L after optimization are both $O(n^2)$, the further calculation of the average eigenvalues $\overline{\lambda}$ is equivalent to calculating the trace of L, which means $O(n)$ and $O(1)$ for time and space complexity, respectively. Not many efficient methods exist for calculating the minimum positive eigenvalue, especially for large-scale and sparse matrices. One class of relatively efficient methods is the Krylov subspace method [42], which has time and space complexities of $O(kn^2)$ and $O(n^2)$ per iteration, respectively, where k is less than n and represents the dimension of the subspace $\mathcal{K}_k(L,b)=\text{span}\{b,Lb,L^2b,\ldots,L^{k-1}b\}$, and the n-dimensional vector b needs to be carefully chosen to ensure that b through $L^{k-1}b$ are k linearly independent basis vectors of $\mathcal{K}_k(L,b)$. In summary, the space-time complexity required to estimate the size and time of model convergence depends mainly on the complexity of computing the eigenvalues of the team topological matrix. However, it should be noted that the above analysis of the computation complexity assumes that the space-time complexity of the two functions f and μ are both $O(1)$. Though the specific forms of f and μ considered in this paper's "Numerical simulation" section meet the assumption, additional analysis is still needed for the case that they have more complex forms.

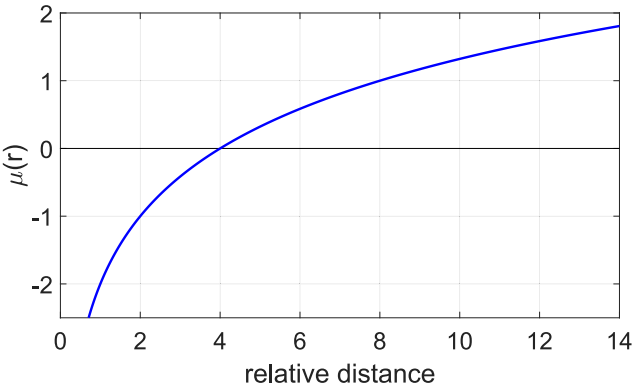

FIGURE 2. Partial image of the attraction/repulsion function between agents in case 1($a=1$, $b=2$, $r_0=4$).

C. PARAMETERS ANALYSIS

1) MINIMUM POSITIVE EIGENVALUE OF SWARM TOPOLOGY'S LAPLACIAN MATRIX

Given that λ_2 plays a pivotal role in the related calculations of model convergence, the specific effects of its changes on the model performance need to be elaborated further. Firstly, the form of the estimated convergence size γ in (25) demonstrates that it decreases monotonically as λ_2 increases, which can be easily proved by finding the partial derivative of γ concerning λ_2. This means that the increases of λ_2 to some extent, hence the convergence of the proposed multi-agent model, and generally speaking, the stronger the convergence, the more stable the system because the fluctuation range of the agent motion also decreases in a smaller convergence space. In addition, the effect of the change in λ_2 on the convergence rate of the model can be deduced from the conclusion of **Theorem 2**.

Theorem 3: For any $\rho_1 > \rho_2 > \frac{1}{2}\gamma_1^2$, the estimated maximum time required for $V(e)$ to converge from ρ_1 to ρ_2 in **Theorem 2** decreases with the increase of λ_2 when other conditions are equal.

Proof: The following derivatives of Δ, γ_1, and γ_2 with respect to λ_2 can be obtained from (27), (28), (29),

TABLE 1. Comparison among various first-order multi-agent systems using the Lyapunov function method for stability analysis.

Ref	Ref[14]	Ref[15]	Ref[27]
Motion Equations	$\dot{x}_i = \sum_{j=1,j\neq i}^{M} g\left(x_i - x_j\right), i,j = 1,\cdots,N$	$\dot{x}_i = -\nabla_{x_i}\sigma\left(x_i\right) + \sum_{j=1,j\neq i}^{M} g\left(x_i - x_j\right), i,j = 1,\cdots,N$	$\dot{x}_i = -\nabla_{x_i}\sigma\left(x_i\right) + \sum_{j=1,j\neq i}^{M} w_{ij} g\left(x_i - x_j\right), i,j = 1,\cdots,N$
Assumptions	$g\left(y\right) = -y\left(a - b\exp\left(-\frac{\|y\|^2}{c}\right)\right)$	1.$g\left(y\right) = -y\left(a - b\exp\left(-\frac{\|y\|^2}{c}\right)\right)$ 2.$\|\nabla_{x_i}\sigma\left(x_i\right)\| \leq \sigma$ 3.$\left[\nabla_{x_i}\sigma\left(x_i\right) - \frac{1}{M}\sum_{j=1}^{M}\nabla_{x_i}\sigma\left(x_i\right)\right]^T e_i \geq A_\sigma\|e_i\|^2$	1.$g\left(y\right) = -y\left(a - \frac{b}{\|y\|^4}\right)$ 2.$\xi_i w_{ij} = \xi_j w_{ji}, \xi_i > 0$ for all i 3.Define symmetric matrix $H = [h_{ij}], h_{ij} = \begin{cases} -\xi_i w_{ij}, i \neq j \\ \sum_{l=1,l\neq i}^{M} \xi_i w_{ij}, i = j \end{cases}$ 4.There exists a constant $\rho > 0$ such that $\left\|x_i - x_j\right\| \geq \rho$ for any time 5.$\sigma\left(y\right) = \frac{1}{2}\|y - c_\sigma\|^2 + b_\sigma$ 6.$\left[\nabla_{x_i}\sigma\left(x_i\right) - \left(\sum_{j=1}^{M}\xi_j\right)^{-1}\sum_{j=1}^{M}\xi_j\sigma\left(x_j\right)\right]^T e_i \geq A_\sigma\|e_i\|^2$, $A_\sigma > -a\gamma_2\|e_i\|^2$, γ_2 is the second smallest eigenvalue of H
Lyapunov Functions	$V_i = \frac{1}{2}e_i^T e_i, e_i = x_i - \frac{1}{M}\sum_{j=1}^{M} x_j$	$V_i = \frac{1}{2}e_i^T e_i, e_i = x_i - \frac{1}{M}\sum_{j=1}^{M} x_j$	$V\left(e\right) = \frac{1}{2}\sum_{i=1}^{M}\xi_i e_i^T e_i, e_i = x_i - \tilde{x}, \tilde{x} = \frac{\sum_{i=1}^{M}\xi_i x_i}{\sum_{i=1}^{M}\xi_i}$
Converged Size	$\|e_i\| \leq \varepsilon = \frac{b}{a}\sqrt{\frac{c}{2}}\exp\left(-\frac{1}{2}\right)$	$\|e_i\| \leq \frac{M-1}{aM}\left[b + \frac{2\overline{\sigma}}{M}\right]$ with assumption 1 and 2 $\|e_i\| \leq \frac{b(M-1)}{aM+A_\sigma}$ with assumption 1 and 3	$\sqrt{\sum_{i=1}^{M}\xi_i\|x_i - \tilde{x}\|^2} \leq b\xi_{\max}\frac{\sum_{i,j=1}^{M}\sqrt{\xi_i}w_{ij}}{(a\gamma_2 + A_\sigma\xi_{\max})\rho^3}$
Converged Time	$t_i \leq -\frac{1}{2a}\ln\left(\frac{\varepsilon^2}{V_i(0)}\right)$	-	$t \leq \frac{\xi_{\max}}{a\gamma_2 + A_\sigma\xi_{\max}}\ln\left(\frac{\sqrt{\sum_{i=1}^{M}\xi_i\|x_i(0) - \tilde{x}\|^2}}{\mu} - 1\right)$
Other Conclutions	$\dot{x}_i \to 0$ when $t \to \infty$	Different σ lead to different behaviors of the swarm.	Other results about the converged size and time with different assumptions of σ.
Ref	**Ref[40]**	**Ref[39]**	**this work**
Motion Equations	$\dot{x}_i = f\left(x_i\right) + \sum_{j=1,j\neq i}^{N} g\left(x_i - x_j\right), i,j = 1,\cdots,N$	$\dot{x}_1 = f\left(x_1\right)$ $\dot{x}_i = f\left(x_i\right) + \sum_{j=1,j\neq i}^{N} w_{ij} g\left(x_i - x_j\right), i = 2,\cdots,N$	$\dot{x}_0 = f\left(x_0\right)$ $\dot{x}_i = \sum_{j=0,j\neq i}^{n} w_{ij} g\left(x_j - x_i\right), i = 1,\cdots,n$
Assumptions	1.$g\left(y\right) = -y\left(a - b\exp\left(-\frac{\|y\|^2}{c}\right)\right)$ 2.There exists a constant $\theta > 0$ such that $\|f\left(x\right) - f\left(y\right)\| \leq \theta\|x - y\|$ 3.$a > \frac{2(N-1)}{N^2}\theta$	1.$g\left(y\right) = -y\left(a - g_r\left(\|y\|\right)\right), g_r\left(\|y\|\right)\|y\| \leq b$ 2.There exists a constant $\theta > 0$ such that $\|f\left(x\right) - f\left(y\right)\| \leq \theta\|x - y\|$ 3.Define an $(N-1)\times(N-1)$ symmetric matrix $H = [h_{ij}]$, $h_{ij} = \begin{cases} \theta - ad_{i+1}, 1 \leq i = j \leq N-1 \\ \frac{a}{2}\left(w_{i+1,j+1} + w_{j+1,i+1}\right), 1 \leq i \neq j \leq N-1 \end{cases}$ where $d_i = \sum_{j=1,j\neq i}^{N} w_{ij}$	1.$g\left(y\right) = y\frac{\mu(\|y\|)}{\|y\|}, \|y\| > 0$ 2.There exists a unique zero point r_0 of μ, $\mu\left(\|y\|\right) < 0$ when $\|y\| < r_0$, $\mu\left(\|y\|\right) > 0$ when $\|y\| > r_0$ 3.There exists a constant $\theta > 0$ such that $\|f\left(x\right)\| \leq \theta$ for x_0 at any time 4.The $n \times n$ symmetric matrix $Y = \left[w_{ij} + w_{ji}\right]$ has connectivity
Lyapunov Functions	$V\left(e\right) = \frac{1}{2}\sum_{i=1}^{N} e_i^T e_i, e_i = x_i - \frac{1}{N}\sum_{j=1}^{N} x_j$	$V\left(e\right) = \frac{1}{2}\sum_{i=2}^{N} e_{i-1}^T e_{i-1}, e_{i-1} = x_i - x_1$	$V\left(e\right) = \frac{1}{2}\sum_{i=1}^{n} e_i^T e_i, e_i = x_i - x_0$
Converged Size	$\frac{1}{N}\sum_{i=1}^{N}\|e_i\|^2 \leq \varepsilon = \frac{b^2 c}{2e\left(a - \frac{2(N-1)\theta}{N^2}\right)^2}$	$\sum_{i=2}^{N}\|e_{i-1}\|^2 \leq \frac{b^2\hat{d}^2(N-1)}{\lambda_{\max}^2(H)}$, where $\hat{d} = \max_{2\leq i\leq N} d_i$	$\sqrt{\sum_{i=1}^{n}\|e_i\|^2} \leq \gamma = \frac{\sqrt{n\beta\overline{d}} + \sqrt{n\beta^2\overline{d}^2 + \left(2\delta r_0 n\overline{\lambda} + 4n\theta\right)\left(v\underline{d} + \alpha\lambda_2\left(1 - \frac{m}{n}\right)\right)}}{2\left(v\underline{d} + \alpha\lambda_2\left(1 - \frac{m}{n}\right)\right)}$
Converged Time	$t \leq \frac{1}{\left(a - \frac{2(N-1)\theta}{N^2}\right)^2}\ln\left(\frac{2V_{i=0}(e)}{N\varepsilon}\right)$	-	$t \leq \frac{1}{2\sqrt{\Delta}}\left[\gamma_1\ln\left(\frac{\sqrt{2\rho_1} - \gamma_1}{\sqrt{2\rho_2} - \gamma_1}\right) + \gamma_2\ln\left(\frac{\sqrt{2\rho_2} - \gamma_2}{\sqrt{2\rho_1} - \gamma_2}\right)\right]$, where t is the time required for $\sum_{i=1}^{n}\|e_i\|^2$ to converge from ρ_1 to ρ_2, the meanings of other parameters have been mentioned in the previous part.
Other Conclutions	other results about the converged size and time when swarm in a noisy environment or agents have limited sensing range	-	The specific impact of each parameter on the model performance and the analysis of the computational complexity.

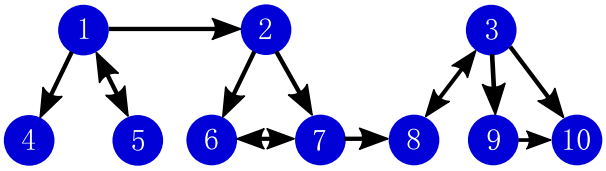

FIGURE 3. Leadership topology of all agents in case 1.

respectively.

$$\frac{d\Delta}{d\lambda_2} = \alpha\left(n - m\right)\left(\frac{1}{2}\delta r_0\overline{\lambda} + \theta\right). \tag{31}$$

$$\begin{aligned}\frac{d\gamma_1}{d\lambda_2} &= \frac{\frac{d\Delta}{d\lambda_2}}{2\sqrt{\Delta}\left(v\underline{d} + \alpha\lambda_2\left(1 - \frac{m}{n}\right)\right)} - \frac{\alpha\left(1 - \frac{m}{n}\right)\left(\frac{1}{2}\sqrt{n}\beta\overline{d} + \sqrt{\Delta}\right)}{\left(v\underline{d} + \alpha\lambda_2\left(1 - \frac{m}{n}\right)\right)^2} \\ &= \frac{\alpha\left(1 - \frac{m}{n}\right)\left(\frac{1}{2}\delta r_0 n\overline{\lambda} + n\theta\right)\left(v\underline{d} + \alpha\lambda_2\left(1 - \frac{m}{n}\right)\right)}{2\sqrt{\Delta}\left(v\underline{d} + \alpha\lambda_2\left(1 - \frac{m}{n}\right)\right)^2} \\ &\quad - \frac{\alpha\left(1 - \frac{m}{n}\right)\left(\sqrt{n\Delta}\beta\overline{d} + 2\Delta\right)}{2\sqrt{\Delta}\left(v\underline{d} + \alpha\lambda_2\left(1 - \frac{m}{n}\right)\right)^2} \\ &= \frac{\alpha\left(1 - \frac{m}{n}\right)\left(\Delta - \frac{1}{4}n\beta^2\overline{d}^2 - \sqrt{n\Delta}\beta\overline{d} - 2\Delta\right)}{2\sqrt{\Delta}\left(v\underline{d} + \alpha\lambda_2\left(1 - \frac{m}{n}\right)\right)^2} \\ &= -\frac{\alpha\left(1 - \frac{m}{n}\right)\left(\frac{1}{2}\sqrt{n}\beta\overline{d} + \sqrt{\Delta}\right)^2}{2\sqrt{\Delta}\left(v\underline{d} + \alpha\lambda_2\left(1 - \frac{m}{n}\right)\right)^2} \\ &= -\frac{\alpha\left(1 - \frac{m}{n}\right)}{2\sqrt{\Delta}}\gamma_1^2 < 0.\end{aligned} \tag{32}$$

$$\begin{aligned}\frac{d\gamma_2}{d\lambda_2} &= \frac{-\frac{d\Delta}{d\lambda_2}}{2\sqrt{\Delta}\left(v\underline{d} + \alpha\lambda_2\left(1 - \frac{m}{n}\right)\right)} - \frac{\alpha\left(1 - \frac{m}{n}\right)\left(\frac{1}{2}\sqrt{n}\beta\overline{d} - \sqrt{\Delta}\right)}{\left(v\underline{d} + \alpha\lambda_2\left(1 - \frac{m}{n}\right)\right)^2} \\ &= -\frac{\alpha\left(1 - \frac{m}{n}\right)\left(\frac{1}{2}\delta r_0 n\overline{\lambda} + n\theta\right)\left(v\underline{d} + \alpha\lambda_2\left(1 - \frac{m}{n}\right)\right)}{2\sqrt{\Delta}\left(v\underline{d} + \alpha\lambda_2\left(1 - \frac{m}{n}\right)\right)^2}\end{aligned}$$

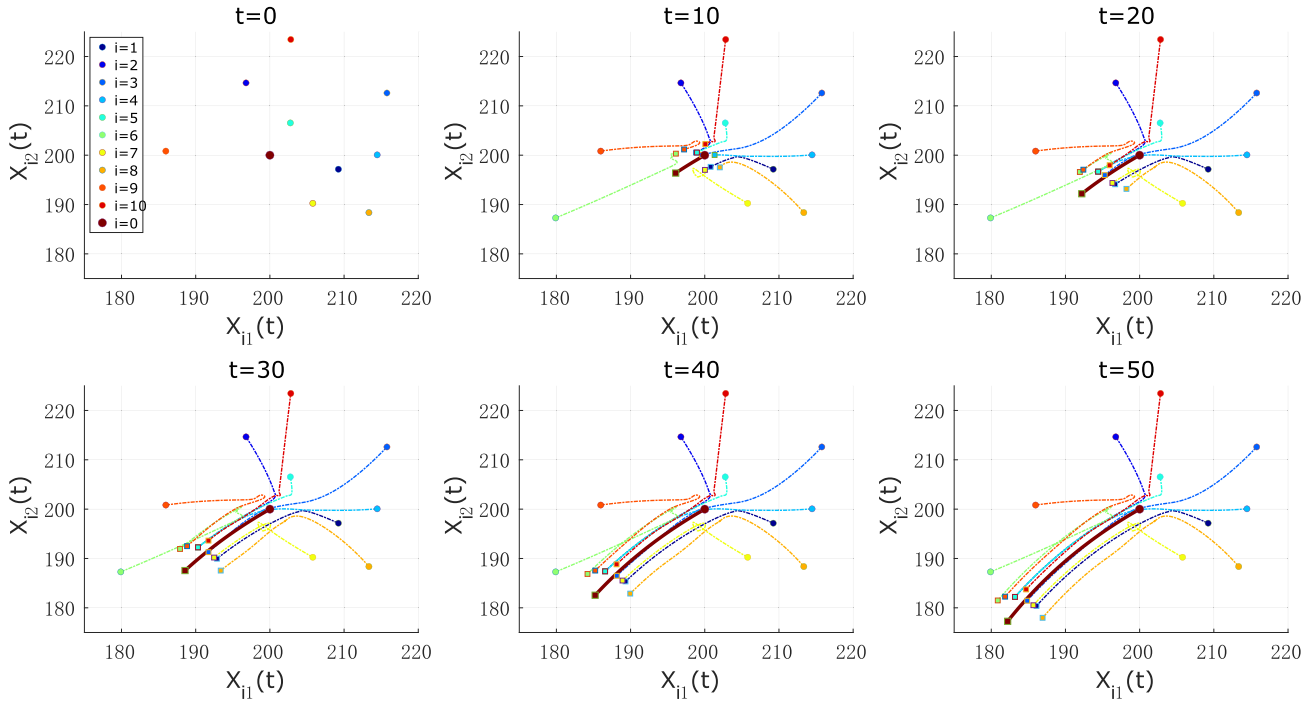

FIGURE 4. The thick solid and thin dashed lines represent the leader's and agents' motion trajectories in case 1 from the initial time to times $t = 0, 10, 20, 30, 40, 50$, respectively. The circles and squares indicate the initial and final positions, respectively.

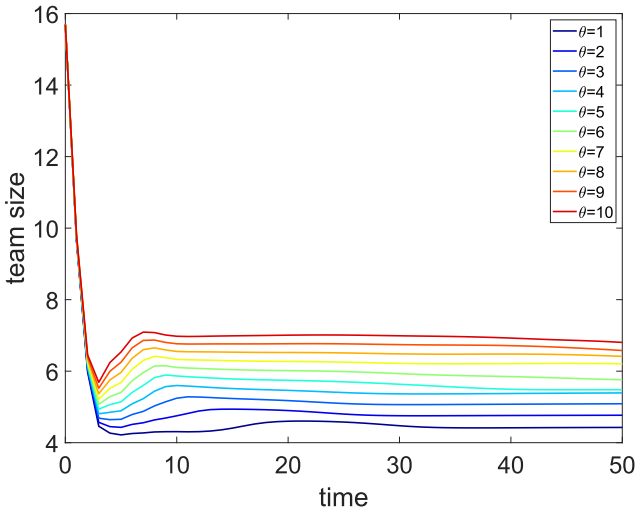

FIGURE 5. The relationship between the trend of swarm size over time during $0 \le t \le 50$ and the θ in case 1.

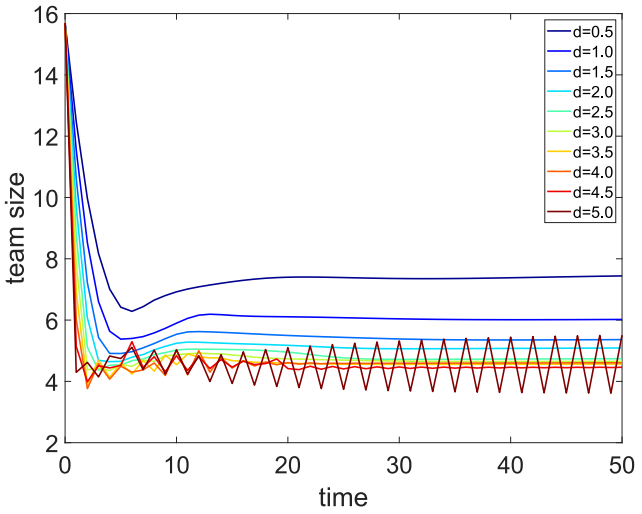

FIGURE 6. The relationship between the trend of swarm size over time during $0 \le t \le 50$ and the d in case 1.

$$
\begin{aligned}
&- \frac{\alpha\left(1-\frac{m}{n}\right)\left(\sqrt{n\Delta}\beta\overline{d}-2\Delta\right)}{2\sqrt{\Delta}\left(v\underline{d}+\alpha\lambda_2\left(1-\frac{m}{n}\right)\right)^2} \\
&= \frac{\alpha\left(1-\frac{m}{n}\right)\left(-\left(\Delta-\frac{1}{4}n\beta^2\overline{d}^2\right)-\sqrt{n\Delta}\beta\overline{d}+2\Delta\right)}{2\sqrt{\Delta}\left(v\underline{d}+\alpha\lambda_2\left(1-\frac{m}{n}\right)\right)^2} \\
&= \frac{\alpha\left(1-\frac{m}{n}\right)\left(\frac{1}{2}\sqrt{n}\beta\overline{d}-\sqrt{\Delta}\right)^2}{2\sqrt{\Delta}\left(v\underline{d}+\alpha\lambda_2\left(1-\frac{m}{n}\right)\right)^2} \\
&= \frac{\alpha\left(1-\frac{m}{n}\right)}{2\sqrt{\Delta}}\gamma_2^2 > 0. \qquad (33)
\end{aligned}
$$

According to the definition of $k(\rho_1, \rho_2)$ in **Theorem 2**, its specific expressions are as follows:

$$
\begin{aligned}
k(\rho_1,\rho_2) &= \frac{\gamma_1 \ln\left(\frac{\sqrt{2\rho_1}-\gamma_1}{\sqrt{2\rho_2}-\gamma_1}\right)+\gamma_2\ln\left(\frac{\sqrt{2\rho_2}-\gamma_2}{\sqrt{2\rho_1}-\gamma_2}\right)}{2\sqrt{\Delta}}, \\
&\rho_1 > \rho_2 > \frac{1}{2}\gamma_1^2 > \frac{1}{2}\gamma_2^2, \quad \gamma_1 > 0 > \gamma_2, \qquad (34)
\end{aligned}
$$

as it is evident that the denominator $2\sqrt{\Delta}$ of k in the above equation is monotonically increasing about λ_2, the negativity of the partial derivative of the function k concerning λ_2 will be determined in the following derivation process only by proving the negativity of the derivative of k's numerator concerning λ_2, namely, proving $\frac{\partial\left(2\sqrt{\Delta}k(\rho_1,\rho_2)\right)}{\partial\lambda_2} < 0$.

$$\begin{aligned}
&\frac{\partial\left(2\sqrt{\Delta}k\left(\rho_1,\rho_2\right)\right)}{\partial\lambda_2}\\
&=\frac{\partial\left(\gamma_1\ln\left(\frac{\sqrt{2\rho_1}-\gamma_1}{\sqrt{2\rho_2}-\gamma_1}\right)+\gamma_2\ln\left(\frac{\sqrt{2\rho_2}-\gamma_2}{\sqrt{2\rho_1}-\gamma_2}\right)\right)}{\partial\lambda_2}\\
&=\frac{d\gamma_1}{d\lambda_2}\left(\ln\left(\frac{\sqrt{2\rho_1}-\gamma_1}{\sqrt{2\rho_2}-\gamma_1}\right)+\frac{\gamma_1\left(\sqrt{2\rho_1}-\sqrt{2\rho_2}\right)}{\left(\sqrt{2\rho_1}-\gamma_1\right)\left(\sqrt{2\rho_2}-\gamma_1\right)}\right)\\
&\quad-\frac{d\gamma_2}{d\lambda_2}\left(\ln\left(\frac{\sqrt{2\rho_1}-\gamma_2}{\sqrt{2\rho_2}-\gamma_2}\right)+\frac{\gamma_2\left(\sqrt{2\rho_1}-\sqrt{2\rho_2}\right)}{\left(\sqrt{2\rho_1}-\gamma_2\right)\left(\sqrt{2\rho_2}-\gamma_2\right)}\right).
\end{aligned}\tag{35}$$

Since $\frac{d\gamma_1}{d\lambda_2} < 0$ and $\frac{d\gamma_2}{d\lambda_2} > 0$ have been proved in (32) and (33), respectively, and parameters in (35) satisfied $\rho_1 > \rho_2 > \frac{1}{2}\gamma_1^2 > \frac{1}{2}\gamma_2^2$. Therefore, $\frac{\partial\left(2\sqrt{\Delta}k(\rho_1,\rho_2)\right)}{\partial\lambda_2} < 0$, which also means $\frac{\partial k(\rho_1,\rho_2)}{\partial\lambda_2} < 0$.

Theorem 3 shows that the smallest positive eigenvalue λ_2 of the swarm topology's Laplacian matrix L characterizing the convergence rate of the multi-agent system, with a larger smallest eigenvalue commonly indicating faster convergence, which is consistent with the conclusions of many previous studies [43], [44], [45], [46], [47], [48]. However, the specific effects of λ_2's changes on the model performance will not be simulated in this paper. A crucial reason is that modifying the matrix to precisely adjust (most of the time maximizing) its minimum eigenvalue is very complex and sufficient to support another paper [49], [50].

2) WEIGHTS OF THE VIRTUAL LEADER'S IMPACT ON ALL AGENTS

In addition to λ_2, the effects of $\overline{d}$ and $\underline{d}$ on the model performance are worth analyzing, since they denote the maximum/minimum weights of the virtual leader's impact on all agents, respectively. However, it is intuitive to observe that their effect on the estimated converged size γ in (25) is opposite, as the growth of $\overline{d}$ increases γ and the opposite for $\underline{d}$. In order to explore the specific effects of the leader's attraction/repulsion weights for agents on the model's performance and simplify the analysis, it is better to assume $\overline{d} = \underline{d} = d > 0$ and let $t = \frac{1}{d}$. Therefore, the partial derivative of γ to t is calculated as follows:

$$\begin{aligned}
&\frac{\partial\gamma}{\partial t}\\
&=\frac{\partial\left(\frac{\sqrt{n}\beta+\sqrt{\nabla}}{2\left(v+\alpha\lambda_2\left(1-\frac{m}{n}\right)t\right)}\right)}{\partial t}\\
&=\frac{2n\left(\delta r_0\bar{\lambda}+2\theta\right)\left(v+2\alpha\lambda_2\left(1-\frac{m}{n}\right)t\right)\left(v+\alpha\lambda_2\left(1-\frac{m}{n}\right)t\right)}{4\sqrt{\nabla}\left(v+\alpha\lambda_2\left(1-\frac{m}{n}\right)t\right)^2}\\
&\quad-\frac{2\alpha\lambda_2\left(1-\frac{m}{n}\right)\left(\sqrt{n}\beta+\sqrt{\nabla}\right)}{4\left(v+\alpha\lambda_2\left(1-\frac{m}{n}\right)t\right)^2}\\
&=\frac{\frac{\nabla-n\beta^2}{t}\left(v+2\alpha\lambda_2\left(1-\frac{m}{n}\right)t\right)}{4\sqrt{\nabla}\left(v+\alpha\lambda_2\left(1-\frac{m}{n}\right)t\right)^2}-\frac{2\alpha\lambda_2\left(1-\frac{m}{n}\right)\left(\sqrt{n}\beta+\sqrt{\nabla}\right)}{4\left(v+\alpha\lambda_2\left(1-\frac{m}{n}\right)t\right)^2}\\
&=\frac{\left(\sqrt{n}\beta+\sqrt{\nabla}\right)\left(\sqrt{\nabla}-\sqrt{n}\beta\right)\left(v+2\alpha\lambda_2\left(1-\frac{m}{n}\right)t\right)}{4\sqrt{\nabla}t\left(v+\alpha\lambda_2\left(1-\frac{m}{n}\right)t\right)^2}\\
&\quad-\frac{\left(\sqrt{n}\beta+\sqrt{\nabla}\right)\alpha\lambda_2 t\left(1-\frac{m}{n}\right)}{2t\left(v+\alpha\lambda_2\left(1-\frac{m}{n}\right)t\right)^2}\\
&=\frac{\left(\sqrt{n}\beta+\sqrt{\nabla}\right)\left(\left(\sqrt{\nabla}-\sqrt{n}\beta\right)v-2\alpha\lambda_2 t\left(1-\frac{m}{n}\right)\sqrt{n}\beta\right)}{4\sqrt{\nabla}t\left(v+\alpha\lambda_2\left(1-\frac{m}{n}\right)t\right)^2},
\end{aligned}\tag{36}$$

where

$$\nabla = n\beta^2 + 2nt\left(\delta r_0\bar{\lambda}+2\theta\right)\left(v+\alpha\lambda_2\left(1-\frac{m}{n}\right)t\right),$$

and the key to determining whether $\frac{\partial\gamma}{\partial t}$ is positive or negative is in the following molecular part of (36):

$$\left(\sqrt{\nabla}-\sqrt{n}\beta\right)v-2\alpha\lambda_2 t\left(1-\frac{m}{n}\right)\sqrt{n}\beta.\tag{37}$$

According to the definition of v, $v = 0$ only if all agents are within equilibrium distance of the leader's attraction/repulsion, which means all agents are subject to a repulsive force from the leader at this time. Therefore, the convergence of the model will be weakened when d increases, which means $\frac{\partial\gamma}{\partial t} < 0$, which is consistent with the positive and negative nature of (37) at $v = 0$. When $v > 0$, the following transformation can be applied to (37):

$$\begin{aligned}
&\left(\sqrt{\nabla}-\sqrt{n}\beta\right)v-2\alpha\lambda_2 t\left(1-\frac{m}{n}\right)\sqrt{n}\beta\\
&=\frac{v\left(\nabla-\left(2\frac{\alpha}{v}\lambda_2 t\left(1-\frac{m}{n}\right)+1\right)^2 n\beta^2\right)}{\sqrt{\nabla}+\left(2\frac{\alpha}{v}\lambda_2 t\left(1-\frac{m}{n}\right)+1\right)\sqrt{n}\beta}\\
&=\frac{2ntv\left(\alpha\lambda_2 t\left(1-\frac{m}{n}\right)+v\right)\left(\delta r_0\bar{\lambda}+2\theta-2\frac{\alpha}{v^2}\lambda_2\left(1-\frac{m}{n}\right)\beta^2\right)}{\sqrt{\nabla}+\left(2\frac{\alpha}{v}\lambda_2 t\left(1-\frac{m}{n}\right)+1\right)\sqrt{n}\beta}.
\end{aligned}\tag{38}$$

Now the key for judging $\frac{\partial\gamma}{\partial t}$ becomes:

$$\delta r_0\bar{\lambda}+2\theta-2\frac{\alpha}{v^2}\lambda_2\left(1-\frac{m}{n}\right)\beta^2.\tag{39}$$

However, it is challenging to draw straightforward conclusions about $\frac{\partial\gamma}{\partial t}$ based on (39) without any specific cases because parameters contained in (39) involving information about the leadership topology of the swarm ($\bar{\lambda}$, λ_2), attraction and repulsion functions (r_0), and the motion equation of the leader (θ), not to mention the four time-varying parameters

which reflect the real-time states of the system (δ, α, v, β). Thus, in practical application scenarios of the model, the calculation of (39) based on the real-time values of the parameters is needed to determine the trend of the effect of d on the convergence of the model.

3) NUMBER OF AGENTS

Besides, it can be easily determined that the convergence size of the model is substantially unaffected by the number of agents n. According to (25), the sum of the squares of the distances from all agents to the leader $\|e\|^2$ eventually does not exceed γ^2, which means:

$$\begin{aligned}&\|e\|^2\\&=\sum_{i=1}^{n}\|e_i\|^2\le\gamma^2\\&=n\left(\frac{\beta\overline{d}+\sqrt{\beta^2\overline{d}^2+\left(2\delta r_0\overline{\lambda}+4\theta\right)\left(v\underline{d}+\alpha\lambda_2\left(1-\frac{m}{n}\right)\right)}}{2\left(v\underline{d}+\alpha\lambda_2\left(1-\frac{m}{n}\right)\right)}\right)^2.\end{aligned}\tag{40}$$

Therefore, the maximum estimated mean of the final distance from each agent to the leader is as follow:

$$\begin{aligned}&\frac{1}{n}\sum_{i=1}^{n}\|e_i\|\\&\le\sqrt{\frac{1}{n}\sum_{i=1}^{n}\|e_i\|^2}\\&\le\frac{\beta\overline{d}+\sqrt{\beta^2\overline{d}^2+\left(2\delta r_0\overline{\lambda}+4\theta\right)\left(v\underline{d}+\alpha\lambda_2\left(1-\frac{m}{n}\right)\right)}}{2\left(v\underline{d}+\alpha\lambda_2\left(1-\frac{m}{n}\right)\right)}.\end{aligned}\tag{41}$$

Since it has been assumed in the proof of **Theorem 1** that $m \ll n$ (between (22) and (23)), the value of (41) is independent of n when the eigenvalue-related parameters $\overline{\lambda}$ and λ_2 do not vary with the size of leadership topology matrix W. It is sufficient to approximately accomplish this by keeping all elements of W (except for the diagonal, the first row, and the first column) identical and inversely proportional to the matrix size n because the eigenvalues of the Laplacian matrix L derived from such matrices W satisfy

$$0=\lambda_1<\lambda_2=\lambda_3=\cdots\cdots=\lambda_n=2nw,$$

which means for fixed $\overline{\lambda}$ and λ_2, the identical elements w of the matrix W remain inversely proportional to the matrix size n. For the whole swarm, this means that all agents are equivalent, the weights of the forces on them (except those exerted by the leader) are evenly distributed among the remaining agents, and each of their total weights does not vary with the number of agents. As a result, for a swarm with the above characteristics, the convergence size is independent of the number of agents. For those swarms with general leadership topologies that do not have this specialization, the effect of agent num on the convergence size will be more complex and not be discussed in this paper.

In summary of the analysis of Section III, a comparison between the proposed multi-agent model and similar first-order multi-agent model of prior works is summarized in Table 1.

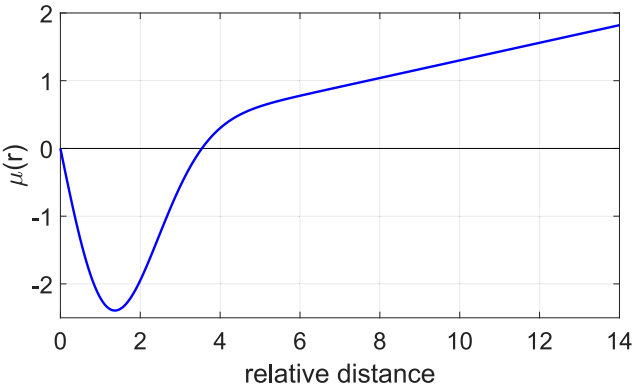

FIGURE 7. Partial image of the attraction/repulsion function between agents in case 2($a = 0.13$, $b = 3$, $c = 4$).

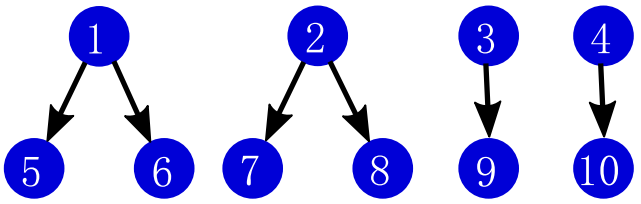

FIGURE 8. Leadership topology of all agents in case 2.

IV. NUMERICAL SIMULATION

This section provides numerical simulations of several cases to illustrate the theoretical analysis. The multi-agent system that contains a virtual leader and ten agents (i.e.$n = 10$, $m = 2$) in a two-dimensional space was considered in the following three cases.

Case 1: The attraction/repulsion function $\mu(y)$ is chosen as the following simple form that satisfies **Assumption 2**

$$\mu(y)=a\log_b\left(\frac{y}{r_0}\right)$$

where the positive constants a and b is used to control the amplitude of μ, and the positive constant r_0 denotes the critical distance at which the attractive and repulsive forces are balanced. Let $a = 1$, $b = 2$, $r_0 = 4$, then the function image of $\mu(y) = \log_2\left(\frac{y}{4}\right)$ is shown in Fig.2.

In order to verify the sufficient condition for convergence of the model in **Theorem 1** that the symmetric matrix Y derived from the coupling matrix W has connectivity, taking $w_{15} = w_{21} = w_{41} = w_{51} = w_{38} = w_{87} = w_{62} = w_{72} = w_{67} = w_{83} = w_{93} = w_{10,3} = w_{76} = w_{10,9} = 1$, and $w_{10} = w_{20} = w_{30} = w_{40} = w_{50} = w_{60} = w_{70} = w_{80} = w_{90} = w_{10,0} = 2$, while all other elements are 0. The leadership topology structure of all agents is shown in Fig.3,

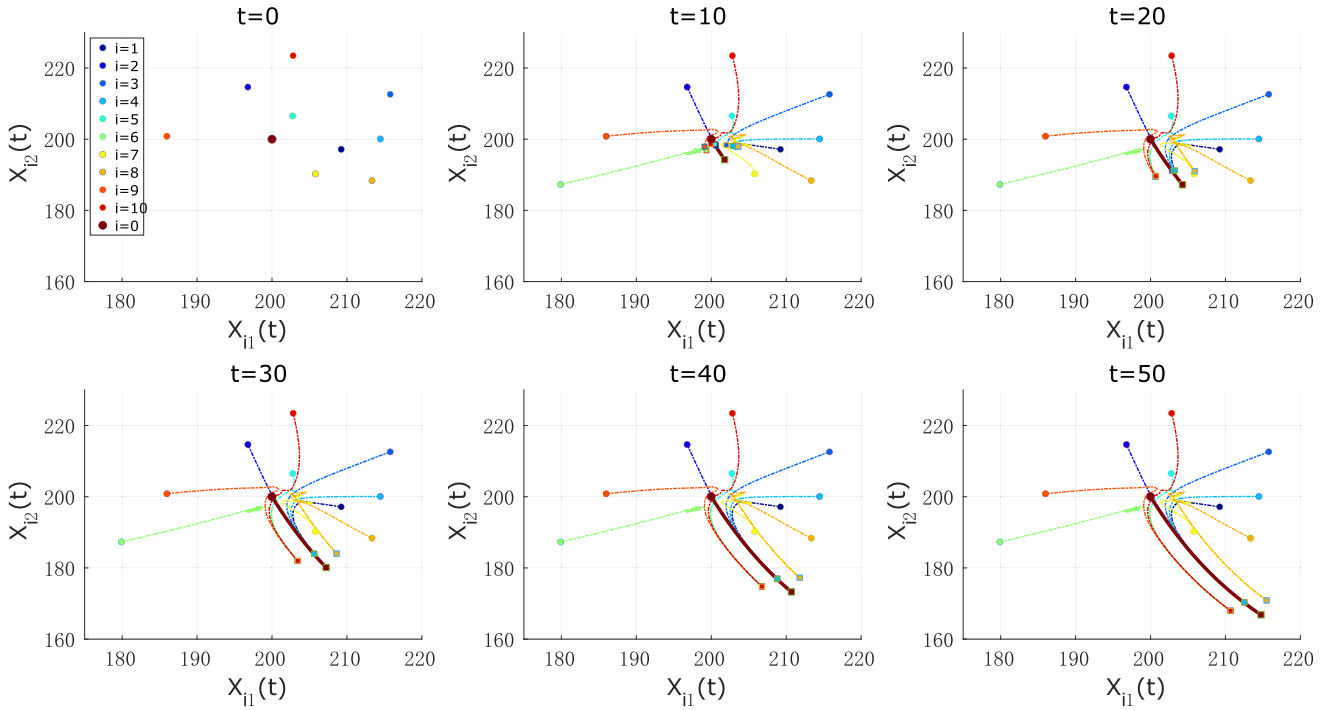

FIGURE 9. The thick solid and thin dashed lines represent the leader's and agents' motion trajectories in case 2 from the initial time to times $t = 0, 10, 20, 30, 40, 50$, respectively. The circles and squares indicate the initial and final positions, respectively.

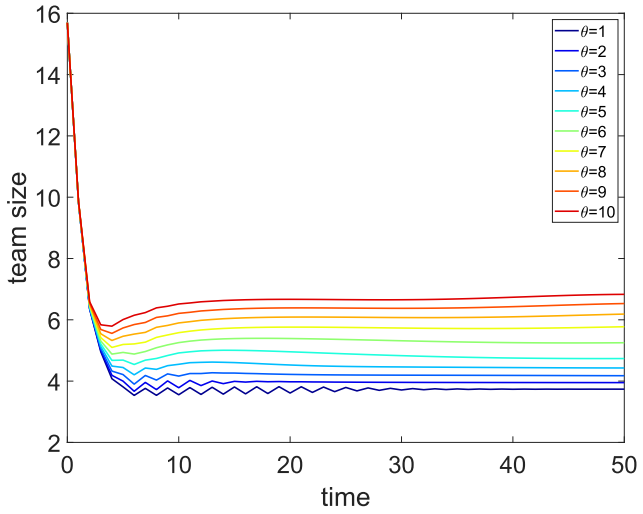

FIGURE 10. The relationship between the trend of swarm size over time during $0 \le t \le 50$ and the θ in case 2.

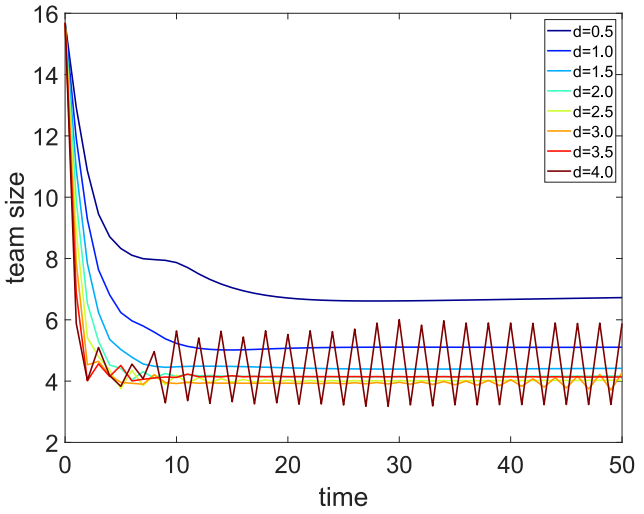

FIGURE 11. The relationship between the trend of swarm size over time during $0 \le t \le 50$ and the d in case 2.

in which the agent at the beginning of each arrow influences the agent at the end.

The nonlinear function f describing the external navigation input and the feedback from real-time swarm size is of the form $f(x_i) = \frac{3}{\sum_{i=1}^{n} \|e_i\|} \left(\sin\left(\frac{x_{i1}}{50}\right), \cos\left(\frac{x_{i2}}{50}\right)\right)$ that satisfies **Assumption 1**, and so $\theta = 3$.

Fig.4 shows the motion trajectories of the virtual leader and all agents in the two-dimensional space, which indicateas that all agents form a cohesive swarm and follow the leader's movement.

Fig.5 shows that the average distance between agents and the leader is affected by θ (from 1 to 10) under the same other conditions, such that the convergence size decreases with the increase in θ, which is consistent with the conclusion of (25).

Fig.6 illustrates the effect of d on the average distance between the leader and the agents (suppose $\overline{d} = \underline{d} = d$ from 0.5 to 5.0) under the same other conditions. It is

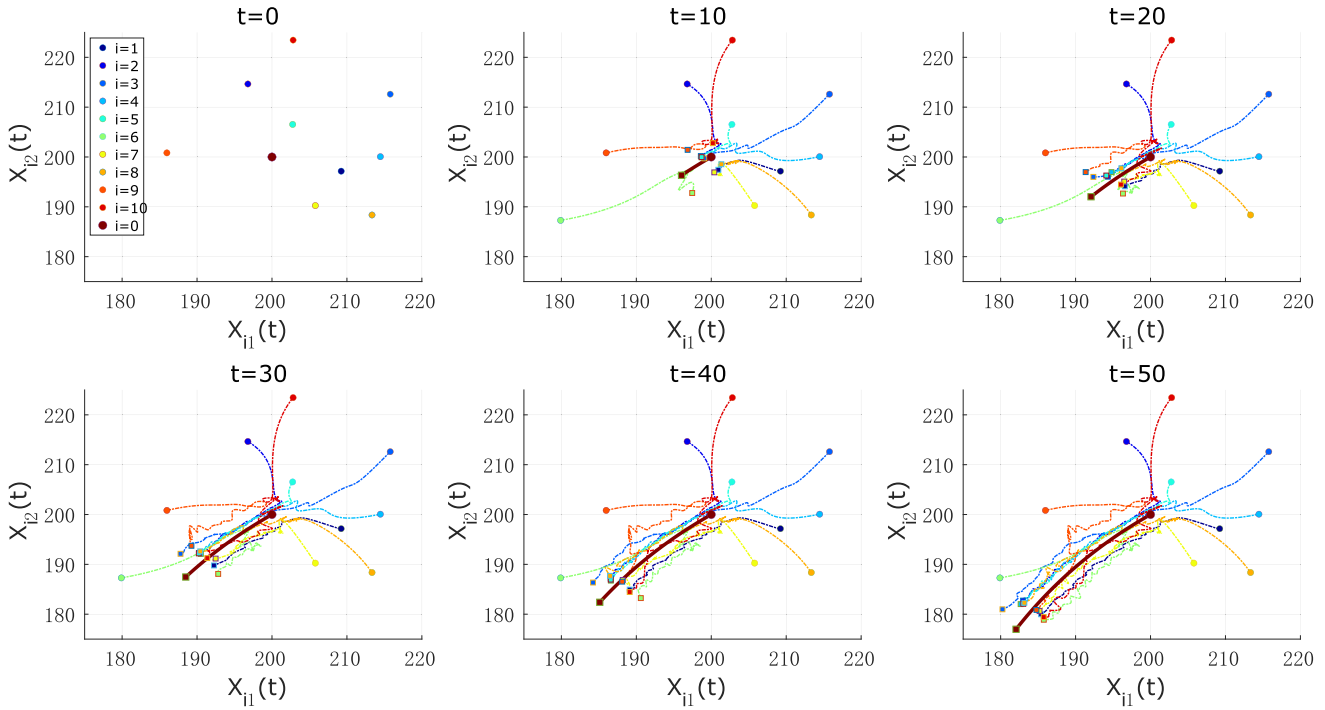

FIGURE 12. The thick solid and thin dashed lines represent the leader's and agents' motion trajectories in case 3 from the initial time to times $t = 0, 10, 20, 30, 40, 50$, respectively. The circles and squares indicate the initial and final positions, respectively.

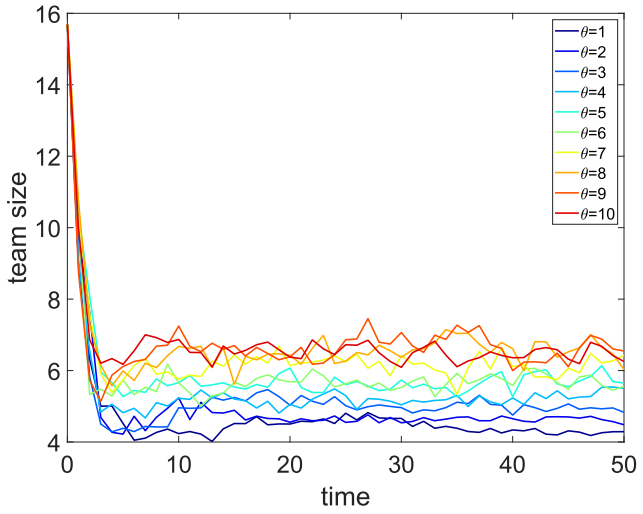

FIGURE 13. The relationship between the trend of swarm size over time during $0 \leq t \leq 50$ and the θ in case 3.

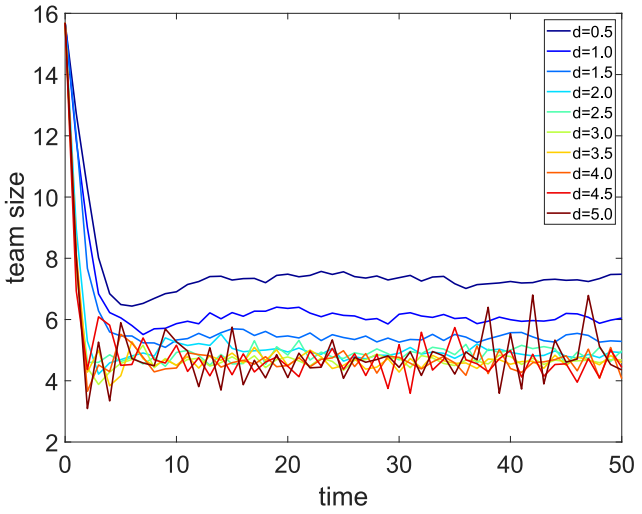

FIGURE 14. The relationship between the trend of swarm size over time during $0 \leq t \leq 50$ and the d in case 3.

demonstrated that a more significant d implies more robust convergence for the model. However, the system oscillates within a specific range when d increases to 5.0, which is due to the leader's overly strong attraction/repulsion effect on the agents, causing the agents to approach the leader too fast and after crossing the equilibrium position dramatically, they are subjected to stronger repulsion and pushed back out of the equilibrium position, and the cycle repeats itself. This phenomenon does not contradict the conclusion of **Theorem 1**, which only indicates that the system converges to a certain range rather than specific behavior in this range.

Case 2: Regarding the attraction/repulsion functions $\mu(y)$ between agents, a common form was usually took in many papers as follows:

$$\mu(y) = y\left(a - b\exp\left(-\frac{y^2}{c}\right)\right)$$

where the positive constants a, b, and c are used to control the amplitude of attraction and repulsion terms, respectively, let

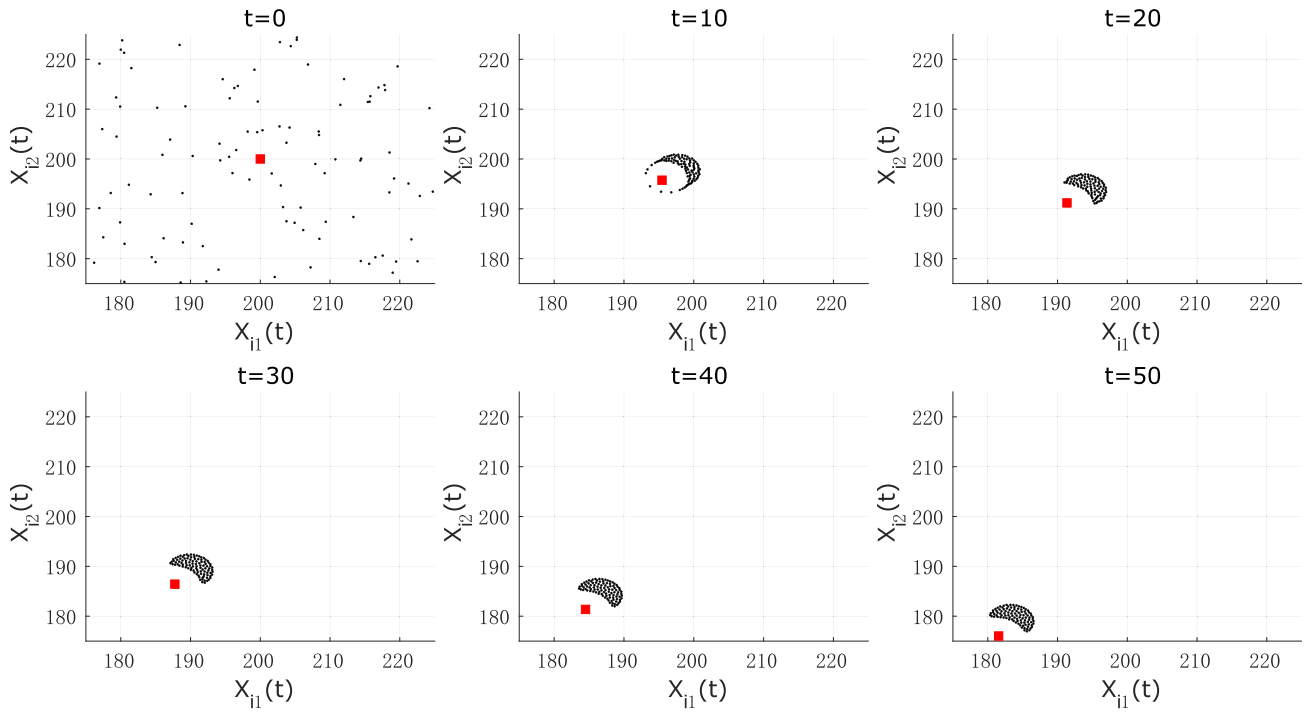

FIGURE 15. Two-dimensional plots of $x_i(t)$, $0 \le i \le 100$ in case 4 at time $t = 0, 10, 20, 30, 40, 50$. The larger red square and the smaller black dots represent the leader and agents, respectively.

$a = 0.13$, $b = 3$, $c = 4$, then the function image of $\mu(y) = y\left(0.13 - 3\exp\left(-\frac{y^2}{4}\right)\right)$ is shown in Fig.7. In contrast to case 1, the non-necessity of condition in **Theorem 1** is verified by depriving the connectivity of Y in this case, thus the positive entries of W are $w_{51} = w_{61} = w_{72} = w_{82} = w_{93} = w_{10,4} = 1$, and $w_{10} = w_{20} = w_{30} = w_{40} = w_{50} = w_{60} = w_{70} = w_{80} = w_{90} = w_{10,0} = 2$. The leadership topology structure of all agents is shown in Fig.8. And the nonlinear function f is now given by $f(x_i) = \frac{3}{\sum_{i=1}^{n} \|e_i\|}\left(\cos\left(\frac{x_{i1}}{40}\right), \sin\left(\frac{x_{i2}}{40}\right)\right)$. Though Y no longer has connectivity, that is, **Assumption 3** is not satisfied. We are about to see that the group with the same initial positions as case 1 still forms a cohesive swarm and follows the leader's motion in the corresponding simulation in Fig.9. From Fig.9, it is seen that there is a phenomenon of overlap among agents due to the convergence of the attraction/repulsion function to the origin. The specifics of the overlap between all agents are determined by their initial positions and the leadership topology.

In analogy to case 1, the swarm bound increases as the parameter θ increases, which can be seen in Fig.10.

Fig.11 is analogous to Fig.6, both reflecting a similar trend in the effect of d on model performance. A slight difference is that since the repulsive force of the attraction/repulsion function of case2 is more severe than that of case1 for most of the interval within the attractive/repulsive equilibrium distance, the oscillation of the system occurs at d = 4.0, and the magnitude is also more extensive than that of case1.

Case 3: According to the previous discussion, a certain degree of randomness exists in the movement of agents in natural multi-agent groups. The accuracy of communication and positioning between agents depends on their relative distance, and the randomness of motion caused by this effect usually increases with the increase of distance, whether in robot formations or biological communities. Therefore, the actual value of $\|g(y)\|$ was randomly taken between $\left(1 - \frac{2}{\pi}\arctan\|y\|\right)\mu(\|y\|)$ and $\left(1 + \frac{2}{\pi}\arctan\|y\|\right)\mu(\|y\|)$ in this case, while other conditions are adopted as in case 1. Two-dimensional plots and trajectories of $x_i(t)$ for $0 \le i \le 10$ and $0 \le t \le 50$ are depicted in Fig.12. Although there are fluctuations in the trajectory of agents compared to case 1, similar swarming and following behavior can still be observed. Moreover, the relationship between swarm size and θ, shown in Fig.13, basically conforms to the same rules as in the first two cases, and so does Fig.14, which demonstrates the relationship between swarm size and d.

Case 4: This case will demonstrate the numerical stability performed when the system scaled up to a much higher number of agents. Consider a reciprocal multi-agent system with one virtual leader and a hundred agents, with the same conditions as in case 1 except for the leadership topology of the swarm. Based on the preconditions used in Section III-C3 for analyzing the number of agents, we are taking all entries of W equal to 0.02 except those in the diagonal, the first row, and the first column. Two-dimensional plots of $x_i(t)$, $0 \le i \le 100$ are depicted in Fig.15, in which the swarming behavior still occurs with the agents on this quantitative scale.

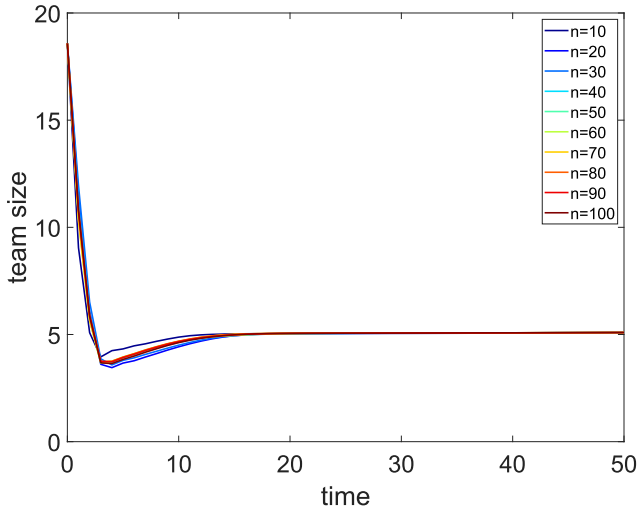

FIGURE 16. The relationship between the trend of swarm size over time during $0 \leq t \leq 50$ and the d in case 3.

Moreover, the relationship between the trend of swarm size over time during $0 \leq t \leq 50$ and the number of agents n are depicted in Fig.16, in which the identical positive entries of W are $\frac{2}{n}$. The results shown in Fig.16 consistent with the analysis in Section III-C3. That is, the convergence size of a reciprocal multi-agent system is independent of the number of agents when the total weight of the force on each agent is identically constant and always evenly distributed among other agents.

V. CONCLUSION

This paper proposes a novel first-order multi-agent model suitable for outdoor group motions and provides stability analysis research results. In this model, only a unique virtual leader with a self-adaptive feedback mechanism can directly perceive external navigation input. At the same time, all agents follow a rooted leadership structure and have inherent nonlinear dynamics that follow the principle of near-repulsion and far-attraction. It is proved that the multi-agent system will ultimately achieve cohesion if a symmetric matrix derived from the coupling topology matrix has connectivity and the repulsion force is indeed bounded. Moreover, the estimates of convergence size and time are obtained. In addition, the computational complexity of the model and the effect of most of the parameters in the model on the model performance were analyzed. Numerical simulations show that the conclusions still apply after introducing a certain degree of motion randomness because flocking and following behaviors occur in the system, which verifies the theoretical results.

Nevertheless, one limitation of this paper is the multi-agent model's rooted leadership property, which guarantees that even if the leadership topology of the swarm changes at some point, this kind of change will not cause the direct or indirect leadership relationship between each agent and the overall leader to disappear. While this direct or indirect leader-following relationship being temporarily weakened and disappears was frequently observed in nature. In that case, more than a single overall leader may be needed to keep the convergence of the swarm since the model's leadership is unrooted, and the stability needs further analysis. Another area for improvement is the ignorance of obstacles that may be common in practical scenarios. Since it defaults that agents are "blind" to environmental information, how to set leaders to guide agents to avoid obstacles needs to be carefully considered. In some complex situations, it may be difficult for a single leader to meet this requirement. Furthermore, the convergence size and time estimated in this paper are very conservative. Thus far, to the best of our knowledge, it is still hard to accurately calculate the convergence results of the stability of multi-agent models. We leave these challenges for our future work.

ACKNOWLEDGMENT

Zhibin Zeng was a visiting scholar (funded by the China Scholarship Council) at the University of Adelaide when this work was done. S. J. Chen and C. Fumeaux are with the School of Electrical and Electronic Engineering, The University of Adelaide, Adelaide, Australia.

REFERENCES

[1] J. H. Reif and H. Wang, "Social potential fields: A distributed behavioral control for autonomous robots," *Robot. Auto. Syst.*, vol. 27, no. 3, pp. 171–194, May 1999.

[2] B. Wang, S. Nersesov, and H. Ashrafiuon, "Formation regulation and tracking control for nonholonomic mobile robot networks using polar coordinates," *IEEE Control Syst. Lett.*, vol. 6, pp. 1909–1914, 2022.

[3] E. Restrepo, A. Loría, I. Sarras, and J. Marzat, "Leader-follower consensus of unicycles with communication range constraints via smooth time-invariant feedback," *IEEE Control Syst. Lett.*, vol. 5, no. 2, pp. 737–742, Apr. 2021.

[4] Q. Wang, H. Dong, B. Ning, L. Y. Wang, and G. Yin, "Two-time-scale hybrid traffic models for pedestrian crowds," *IEEE Trans. Intell. Transp. Syst.*, vol. 19, no. 11, pp. 3449–3460, Nov. 2018.

[5] A. Tordeux, M. Chraibi, and A. Seyfried, "Collision-free speed model for pedestrian dynamics," in *Traffic and Granular Flow '15*, V. L. Knoop and W. Daamen, Eds. Cham, Switzerland: Springer, 2016, pp. 225–232.

[6] Q. Xu, M. Chraibi, A. Tordeux, and J. Zhang, "Generalized collision-free velocity model for pedestrian dynamics," *Phys. A, Stat. Mech. Appl.*, vol. 535, Dec. 2019, Art. no. 122521.

[7] R.-Y. Guo, S. C. Wong, H.-J. Huang, P. Zhang, and W. H. K. Lam, "A microscopic pedestrian-simulation model and its application to intersecting flows," *Phys. A, Stat. Mech. Appl.*, vol. 389, no. 3, pp. 515–526, Feb. 2010.

[8] S.-L. Dai, S. He, X. Chen, and X. Jin, "Adaptive leader-follower formation control of nonholonomic mobile robots with prescribed transient and steady-state performance," *IEEE Trans. Ind. Informat.*, vol. 16, no. 6, pp. 3662–3671, Jun. 2020.

[9] Y. Xu, Z. Wang, and J. Chen, "Formation tracking control for multi-agent systems on directed graphs," in *Proc. Chin. Control Conf. (CCC)*, Jul. 2019, pp. 47–52.

[10] Q. Yao, Z. Zheng, L. Qi, H. Yuan, X. Guo, M. Zhao, Z. Liu, and T. Yang, "Path planning method with improved artificial potential field—A reinforcement learning perspective," *IEEE Access*, vol. 8, pp. 135513–135523, 2020.

[11] Y. Ma, Y. Liu, L. Zhao, and M. Zhao, "A review on cooperative control problems of multi-agent systems," in *Proc. 41st Chin. Control Conf. (CCC)*, Jul. 2022, pp. 4831–4836.

[12] Y. Hou, M. Sun, Y. Zeng, Y.-S. Ong, Y. Jin, H. Ge, and Q. Zhang, "A multi-agent cooperative learning system with evolution of social roles," *IEEE Trans. Evol. Comput.*, early access, pp. 1–14, 2023.

[13] C. W. Reynolds, "Flocks, herds and schools: A distributed behavioral model," in *Proc. 14th Annu. Conf. Comput. Graph. Interact. Techn.*, Aug. 1987, pp. 25–34.
[14] V. Gazi and K. M. Passino, "Stability analysis of swarms," *IEEE Trans. Autom. Control*, vol. 48, no. 4, pp. 692–697, Apr. 2003.
[15] V. Gazi and K. M. Passino, "Stability analysis of social foraging swarms," *IEEE Trans. Syst., Man Cybern., B, Cybern.*, vol. 34, no. 1, pp. 539–557, Feb. 2004.
[16] R. Olfati-Saber, "Flocking for multi-agent dynamic systems: Algorithms and theory," *IEEE Trans. Autom. Control*, vol. 51, no. 3, pp. 401–420, Mar. 2006.
[17] T. Kolokolnikov, H. Sun, D. Uminsky, and A. L. Bertozzi, "Stability of ring patterns arising from two-dimensional particle interactions," *Phys. Rev. E, Stat. Phys. Plasmas Fluids Relat. Interdiscip. Top.*, vol. 84, no. 1, Jul. 2011, Art. no. 015203.
[18] G. Albi, D. Balagué, J. A. Carrillo, and J. von Brecht, "Stability analysis of flock and mill rings for second order models in swarming," *SIAM J. Appl. Math.*, vol. 74, no. 3, pp. 794–818, Jan. 2014.
[19] J. A. Carrillo, Y. Huang, and S. Martin, "Nonlinear stability of flock solutions in second-order swarming models," *Nonlinear Anal., Real World Appl.*, vol. 17, pp. 332–343, Jun. 2014.
[20] J. Qin, Q. Ma, P. Yi, and L. Wang, "Multiagent interval consensus with flocking dynamics," *IEEE Trans. Autom. Control*, vol. 67, no. 8, pp. 3965–3980, Aug. 2022.
[21] Q. Liu, L. Wang, and X. Liao, "Stability analysis of swarms with interaction time delays," *Inf. Sci.*, vol. 192, pp. 244–254, Jun. 2012.
[22] Z. Yang, X. Pan, Q. Zhang, and Z. Chen, "Distributed optimization for multi-agent systems with time delay," *IEEE Access*, vol. 8, pp. 123019–123025, 2020.
[23] J. Yuan, G. Jiang, and X.-B. Chen, "Flocking with informed agents based on incomplete information," *IEEE Access*, vol. 10, pp. 87069–87082, 2022.
[24] S. Das, U. Halder, and D. Maity, "Chaotic dynamics in social foraging swarms—An analysis," *IEEE Trans. Syst., Man, Cybern., B, Cybern.*, vol. 42, no. 4, pp. 1288–1293, Aug. 2012.
[25] S. Das, "Chaotic patterns in the discrete-time dynamics of social foraging swarms with attractant-repellent profiles: An analysis," *Nonlinear Dyn.*, vol. 82, no. 3, pp. 1399–1417, Nov. 2015.
[26] S. Das, D. Goswami, S. Chatterjee, and S. Mukherjee, "Stability and chaos analysis of a novel swarm dynamics with applications to multi-agent systems," *Eng. Appl. Artif. Intell.*, vol. 30, pp. 189–198, Apr. 2014.
[27] B. Liu, T. Chu, L. Wang, and Z. Wang, "Collective motion of a class of social foraging swarms," *Chaos, Solitons Fractals*, vol. 38, no. 1, pp. 277–292, Oct. 2008.
[28] W. Li, "Stability analysis of swarms with general topology," *IEEE Trans. Syst., Man, Cybern., B, Cybern.*, vol. 38, no. 4, pp. 1084–1097, Aug. 2008.
[29] I. D. Couzin, J. Krause, N. R. Franks, and S. A. Levin, "Effective leadership and decision-making in animal groups on the move," *Nature*, vol. 433, no. 7025, pp. 513–516, Feb. 2005.
[30] M. Nagy, Z. Ákos, D. Biro, and T. Vicsek, "Hierarchical group dynamics in pigeon flocks," *Nature*, vol. 464, no. 7290, pp. 890–893, Apr. 2010.
[31] J. Shen, "Cucker–Smale flocking under hierarchical leadership," *SIAM J. Appl. Math.*, vol. 68, no. 3, pp. 694–719, Jan. 2008.
[32] Z. Li and X. Xue, "Cucker–Smale flocking under rooted leadership with fixed and switching topologies," *SIAM J. Appl. Math.*, vol. 70, no. 8, pp. 3156–3174, Jan. 2010.
[33] Z. Li and X. Xue, "Cucker–Smale flocking under rooted leadership with free-will agents," *Phys. A, Stat. Mech. Appl.*, vol. 410, pp. 205–217, Sep. 2014.
[34] F. Dalmao and E. Mordecki, "Cucker–Smale flocking under hierarchical leadership and random interactions," *SIAM J. Appl. Math.*, vol. 71, no. 4, pp. 1307–1316, Jan. 2011.
[35] J. Dong, "Flocking under hierarchical leadership with a free-will leader," *Int. J. Robust Nonlinear Control*, vol. 23, no. 16, pp. 1891–1898, Nov. 2013.
[36] C.-H. Li and S.-Y. Yang, "A new discrete Cucker–Smale flocking model under hierarchical leadership," *Discrete Continuous Dyn. Syst. B*, vol. 21, no. 8, pp. 2587–2599, Sep. 2016.
[37] Z. Li, "Effectual leadership in flocks with hierarchy and individual preference," *Discrete Continuous Dyn. Syst. A*, vol. 34, no. 9, pp. 3683–3702, 2014.
[38] Z. Li, S.-Y. Ha, and X. Xue, "Emergent phenomena in an ensemble of Cucker–Smale particles under joint rooted leadership," *Math. Models Methods Appl. Sci.*, vol. 24, no. 7, pp. 1389–1419, Jun. 2014.
[39] C.-H. Li, "Stability analysis of a swarm model with rooted leadership," *Phys. Lett. A*, vol. 383, no. 1, pp. 1–9, Jan. 2019.
[40] W. Yu, G. Chen, M. Cao, J. Lü, and H.-T. Zhang, "Swarming behaviors in multi-agent systems with nonlinear dynamics," *Chaos, Interdiscipl. J. Nonlinear Sci.*, vol. 23, no. 4, Nov. 2013, Art. no. 043118.
[41] R. A. Horn and C. R. Johnson, *Matrix Analysis*. Cambridge, U.K.: Cambridge Univ. Press, 2012.
[42] J. Liesen and Z. Strakos. *Krylov Subspace Methods: Principles and Analysis* (Numerical Mathematics and Scientific Computation). Oxford, U.K.: Oxford Univ. Press, 2013.
[43] R. Olfati-Saber and R. M. Murray, "Consensus problems in networks of agents with switching topology and time-delays," *IEEE Trans. Autom. Control*, vol. 49, no. 9, pp. 1520–1533, Sep. 2004.
[44] A. Rahmani, M. Ji, M. Mesbahi, and M. Egerstedt, "Controllability of multi-agent systems from a graph-theoretic perspective," *SIAM J. Control Optim.*, vol. 48, no. 1, pp. 162–186, Jan. 2009.
[45] M. Pirani and S. Sundaram, "On the smallest eigenvalue of grounded Laplacian matrices," *IEEE Trans. Autom. Control*, vol. 61, no. 2, pp. 509–514, Feb. 2016.
[46] D. Zelazo and M. Bürger, "On the robustness of uncertain consensus networks," *IEEE Trans. Control Netw. Syst.*, vol. 4, no. 2, pp. 170–178, Jun. 2017.
[47] H. Liu, X. Xu, J.-A. Lu, G. Chen, and Z. Zeng, "Optimizing pinning control of complex dynamical networks based on spectral properties of grounded Laplacian matrices," *IEEE Trans. Syst., Man, Cybern., Syst.*, vol. 51, no. 2, pp. 786–796, Feb. 2021.
[48] B. Wang, H. Liu, J. Xu, and J. Liu, "Pining control algorithm for complex networks," in *Proc. Chin. Control Conf. (CCC)*, Jul. 2019, pp. 964–969.
[49] A. Clark, Q. Hou, L. Bushnell, and R. Poovendran, "Maximizing the smallest eigenvalue of a symmetric matrix: A submodular optimization approach," *Automatica*, vol. 95, pp. 446–454, Sep. 2018.
[50] X. Zhou, H. Sun, W. Li, and Z. Zhang, "Optimization on the smallest eigenvalue of grounded Laplacian matrix via edge addition," *Theor. Comput. Sci.*, vol. 980, Nov. 2023, Art. no. 114220.

ZHIBIN ZENG (Member, IEEE) received the B.E. degree in information engineering from the Wuhan Technical University of Surveying and Mapping, Wuhan, China, in 1998, and the M.E. degree in information and communication engineering and the Ph.D. degree in electronic science and technology from Xidian University, Xi'an, China, in 2004 and 2010, respectively. Since 2011, he has been an Associate Professor with the School of Microelectronics, Xidian University. His current research interests include design of embedded systems, wireless communication, high-speed signal processing, and signal integrity.

ZILUO XIE received the B.E. degree in information engineering from the Hefei University of Technology, Anhui, China, in 2021. He is currently pursuing the master's degree with the School of Microelectronics, Xidian University. His current research interests include the design of embedded systems, wireless communication, and multi-agent systems.

ZHENYU JIANG received the B.E. degree in electronical information science and technology from the Shaanxi University of Science and Technology, Xi'an, China, in 2022. He is currently pursuing the master's degree with the School of Microelectronics, Xidian University. His current research interests include digital IC and the design of system-on-chip.